Research Square

Preprints are preliminary reports that have not undergone peer review.
They should not be considered conclusive, used to inform clinical practice,
or referenced by the media as validated information.

A gravity search algorithm with a distance-fitness evaluation strategy for path planning

Zhichao Feng
Guilin Institute of Information Technology
Jian Sui
Guilin Institute of Information Technology
Zhenzhen Luo
luozhenzhen92@163.com
Guilin Institute of Information Technology

Research Article

Keywords: Gravity search algorithm, Optimization, Benchmark functions, The unmanned aerial vehicle path planning problem

Posted Date: November 5th, 2026

DOI: https://doi.org/10.21203/rs.3.rs-11449983/v1

License: This work is licensed under a Creative Commons Attribution 4.0 International License.
Read Full License

Additional Declarations: No competing interests reported.

A gravity search algorithm with a distance-fitness evaluation strategy for path planning

Zhichao Feng[a], Jian Sui[a], Zhenzhen Luo[a,*]

[a]College of Electronic Engineering, Guilin Institute of Information Technology, Guilin 541100, Guangxi, China

*Corresponding author.

E-mail address: luozhenzhen92@163.com (Zhenzhen Luo)

Abstract: gravity Search Algorithm (GSA) is a swarm intelligence optimization algorithm inspired by Newton's law of universal gravitation. It uses particle masses and interparticle gravity forces to transmit information and evolve candidate solutions. Although the traditional GSA has been successfully applied in several fields, it still suffers from premature convergence and limited search capability when solving complex optimization problems. To address these limitations, this paper proposes a GSA with a self-adaptive attenuation factor and a distance-fitness evaluation strategy, termed SDGSA. The self-adaptive attenuation factor regulates the decay rate of the gravity constant, thereby improving the balance between exploration and exploitation. The distance-fitness evaluation strategy assesses both the spatial distances and fitness values of individuals, allowing the algorithm to adapt its search to the population distribution. This strategy increases population diversity and reduces the likelihood of becoming trapped in local optima. SDGSA is evaluated against several GSA variants and other metaheuristic algorithms on 58 benchmark functions and an unmanned aerial vehicle

(UAV) path-planning problem. The benchmark results show that SDGSA outperforms its competitors. It also achieves high accuracy on challenging optimization problems.

Keywords: Gravity search algorithm; Optimization; Benchmark functions; The unmanned aerial vehicle path planning problem.

1. Introduction

Optimization problems in scientific research and engineering practice are becoming increasingly complex, as they typically involve a large number of decision variables, complex nonlinear constraints, and higher dimensional objective functions [1]. The search performance and efficiency deteriorate when traditional methods are used to solve optimization problems, especially when the objective functions or constraints have multiple optima. Evolutionary algorithms are powerful tools for solving such complex optimization problems [2]. In addition, with the increasing demand for large-scale optimization, dynamic optimization, and multi-objective optimization, how to improve the efficiency, robustness, and accuracy of evolutionary algorithms remains an important challenge in the field of computational intelligence.

The Gravity Search Algorithm (GSA) is an excellent metaheuristic method inspired by the law of gravity between atoms [3]. On the one hand, due to its powerful search capability, GSA has been widely applied in various engineering fields; on the other hand, as the complexity of the problem to be solved increases, the algorithm still suffers from premature convergence and a sharp decline in search accuracy [4]. A new hybrid swarm algorithm

(PSOGSA) was presented in [5], which combines the exploration ability of PSO with the exploitation ability of GSA to balance exploration and exploitation. Lei et al. [6] proposed a new aggregation learning gravity search algorithm (ALGSA) which introduced an adaptive gravity constant into the algorithm to improve the search efficiency of algorithms. An improved gravity search algorithm (IGSA) was proposed [7], which was combined with simulated annealing. Aditya et al. [8] proposed an adaptive gravity search algorithm (DCGSA) for optimizing mechanical engineering design and processing problems. DCGSA introduces an adaptive gravity constant that varies with the level of population diversity. A mixed attraction and repulsion based gravity search algorithm (MAR-GSA) was presented in [9], which was introduced into the algorithm to standardize fitness through quality adjustment, thereby combining the effects of attraction and repulsion. Guo et al. [10] proposed an adaptive position guided gravity search algorithm that determines motion from the best, worst, and remaining particles. Joshi [11] proposed a GSA variant that incorporates chaos-embedded opposition-based learning into the basic GSA for the stagnation-free search. In addition, the algorithm also introduces chaotic gravity constants based on sine and cosine functions. Dikshit [12] proposed a restart-mechanism-based multilevel gravity search algorithm. This algorithm introduces winner-take-all learning to balance exploration and exploitation. It performs restarts through estimation and variation to avoid stagnation and maintain diversity. A hierarchical GSA algorithm (HGSA) with high efficiency was proposed [13]. HGSA establishes a three-tier structure comprising a top layer, middle layer, and bottom layer, enabling hierarchical control from the top layer to the middle layer and from the middle layer to the bottom layer. The most outstanding individuals within the algorithm guide the entire population's evolutionary process.

Ji et al. [14] proposed a self-adaptive gravity search algorithm that introduces an adaptive G value to balance exploration and exploitation. Mittal et al. [15] proposed a peak gravity search algorithm (SGSA) that introduces the "peak effect" to optimize the balance between exploration and exploitation during the process. An adaptive gbest-guided gravity search algorithm (GGSA) was proposed [16], which records and utilizes the location of optimal quality to speed up the search process.

Although all the aforementioned approaches have improved the performance of the GSA algorithm, certain limitations remain. Specifically, most existing GSA variants use the best solution found to date as a guide during the speed update process. Research has confirmed that while introducing the optimal solution can improve search accuracy and accelerate convergence speed, it comes at the cost of rapidly diminishing population diversity. In fact, when addressing complex problems, it is essential to increase or maintain population diversity to prevent premature convergence. Therefore, a gravity search algorithm with self-adapting attenuation factor and distance-fitness evaluation strategy (SDGSA) is proposed to solve these problems. Specifically, SDGSA introduces a distance fitness evaluation strategy, which considers both fitness value and particle distance when evaluating the quality of a solution. The distance-fitness evaluation strategy uses individual historical optimal solutions and Mahalanobis distance. High quality historical location information can guide the population to evolve in a more promising direction, while the Mahalanobis distance can better identify sparse areas. In this strategy, SDGSA can select a balanced individual that both exploits high-quality information and offers exploration potential. The algorithm can use either the balanced individual or the global optimum for updating, rather than relying solely on global optimal

solutions to guide updates. The distance-fitness evaluation strategy can effectively improve the situation where algorithms are prone to falling into local optima and maintain algorithm diversity. In addition, the generation of the gravity constant is regulated through nonlinear attenuation coefficients, aiming to balance the relationship between exploration and exploitation of the algorithm. To evaluate the performance of the SDGSA algorithm, it is compared with three GSA algorithms and 11 efficient metaheuristic optimizers on 58 benchmark problems in two independent test sets. The feasibility and applicability of the developed SDGSA algorithm in practical applications are further verified through two drone path planning cases.

The main contributions of this paper can be outlined as follows:

(1) This article proposes an adaptive attenuation factor suitable for GSA, which is used to adjust the generation of gravity constants, thereby achieving a more reasonable balance between exploration and exploitation of the algorithm.

(2) A distance-fitness evaluation strategy is designed in this study, which can effectively maintain population diversity while reducing the probability of the algorithm falling into local optima.

(3) The proposed SDGSA is used to solve a complex unmanned aerial vehicle (UAV) path planning problem.

2. Conventional gravity search algorithm

GSA is a population-based algorithm inspired by Newton's law of universal gravitation. By utilizing the gravity and mass of individuals within the population, information is

transmitted between individuals and the population is guided to conduct intelligent optimization searches.

Each population contains N particles, and the position of each particle represents a solution. The influence of gravity on individuals is reflected through their mass (expressed in the form of fitness functions), particle spacing, and gravity constant. The gravity interaction between individuals will guide them to move towards individuals with larger mass—the larger the mass, the higher the fitness value. Therefore, the movement direction of each individual reflects its evolution from a low-quality solution to a high-quality solution.

$$m_i(t) = \frac{fitness_i(t) - fitness_{worst}(t)}{fitness_{best}(t) - fitness_{worst}(t)} \tag{1}$$

where $fitness_i(t)$ represent the fitness value of the i-th individual in the t-th iteration, $fitness_{best}(t)$ and $fitness_{worst}(t)$ respectively represent the best fitness value and worst fitness value of all particles in the t-th iteration. The mass $M_i(t)$ of individual $x_i(t)$ is formulated as follows:

$$M_i(t) = \frac{m_i(t)}{\sum_{q=1}^{N} m_q(t)} \tag{2}$$

For an individual, the whole gravity forcefrom other individuals in the t-th iteration is calculated as follows:

$$F_{ij}(t) = \frac{M_i(t) \times M_j(t)}{R_{ij}(t) + \varepsilon}(x_j(t) - x_i(t)) \tag{3}$$

Where $R_{ij}(t)$ is the Euclidean distance between particles i and j at iteration t and ε is a small constant. $G(t)$ is the gravity constant that decreases with iterations, expressed as:

$$G(t) = G_0 \times e^{-a \cdot \frac{t}{T}} \tag{4}$$

where G_0 is an initial value and a is a constant. t and T indicate the current iteration number and the maximum iteration number, respectively. For an individual, the whole gravity force $F_i(t)$ from other individuals in the t-th iteration is calculated as follows:

$$F_i(t) = \sum_{j \in Kbest, j \neq i} rand_j \cdot F_{ij}(t) \tag{5}$$

where *Kbest* is the set of the K particles with the best fitness values in the current population at iteration t. $rand_j$ is a random number distributed between 0 and 1. The acceleration of particle i is calculated as follows:

$$a_i(t) = \frac{F_i(t)}{M_i(t)} \tag{6}$$

Finally, the velocity $v_i(t+1)$ of individual x_i is updated to change its position in the next iteration t+1, given as follows:

$$v_i(t+1) = rand(0,1) \cdot v_i(t) + a_i(t) \tag{7}$$

$$x_i(t+1) = x_i(t) + v_i(t+1) \tag{8}$$

where $v_i(t)$ represents the velocity of the i-th individual at iteration t, $a_i(t)$ represents the acceleration of the i-th individual at iteration t, and $x_i(t)$ represents the position of the i-th individual at iteration *t, respectively.*

3. The proposed SDGSA algorithm

GSA is an efficient and promising algorithm. However, its performance is limited by its underlying mechanisms: the algorithm is prone to premature convergence and has weak search capabilities. The reason is that GSA utilizes the interaction information between individuals in the entire population to continuously generate new individuals, and the movement speed of individuals is controlled by their gravity and mass [17]. During the entire search process, if a

particle falls into a local optimal solution and cannot escape, other particles will also converge to that local optimal solution, and ultimately the entire population will converge to it. In the later stage of search, the speed update value of individuals becomes extremely small, resulting in lower exploration ability when searching for better solutions, which means that the efficiency of update operations used to further optimize the search space is low. Therefore, balancing the search capability of GSA between exploration and exploitation is crucial, as it can continuously improve its performance from the beginning to the end of the optimization process. Therefore, this article proposes a gravity search algorithm based on adaptive attenuation factor and distance-fitness evaluation strategy (SDGSA), aiming to achieve a good balance between exploration and exploitation.

3.1. Self-adapting attenuation factors

In the classical GSA, $G(t)$ monotonically decreases in an exponential form as shown in equation (4)，with its decay rate controlled by a fixed coefficient a. This fixed attenuation strategy has obvious defects: If the value of a is too large and $G(t)$ decays rapidly, the algorithm will lose its global exploration capability during the early stages of the iterative process and will easily become trapped in local optima. If the value of a is too small, convergence is slow, resulting in substantial computational waste. More importantly, the fixed attenuation cannot be dynamically adjusted according to the actual search state of the population, which makes it difficult for the algorithm to maintain the balance between exploration and exploitation in different optimization stages. To solve the above problems, this paper designs an adaptive attenuation factor, whose expression is as follows:

$$a_t = 20 \cdot \tanh\left(\frac{t - T/2}{L}\right) \tag{9}$$

Where tanh is the hyperbolic tangent function, t is the number of iterations, and T is the maximum number of iterations. L is the influence parameter, which controls the shape of the attenuation curve. From equation (9), it can be seen that the value of a_t is small in the initial stage of the iterations, at which $G(t)$ decays slowly, which is conducive to maintaining a strong global search ability. As the iteration proceeds, a_t gradually increases, and $G(t)$ accelerates the attenuation, thus promoting the transition of the algorithm to local fine exploitation. By adjusting L, the change curve of attenuation speed can be flexibly controlled to meet the optimization requirements of different problems. Based on the above adaptive attenuation factor, the update method of gravity constant is redefined as follows:

$$G(t) = G_0 \cdot \exp(-a_t \cdot \frac{t}{T}) \tag{10}$$

Where, G_0 is the initial gravity constant, which is consistent with equation (4). Comparing equation (4) with equation (10), it can be seen that the exponential attenuation coefficient of $G(t)$ in the new strategy is no longer a fixed constant, but the exponential attenuation coefficient of a_t that changes dynamically with iteration. If a_t is large, $G(t)$ decays slowly, and the algorithm focuses on exploring the unknown region. If a_t is small, $G(t)$ rapidly decreases, and the algorithm focuses on using the discovered high-quality regions for local search. This adaptive mechanism enables the algorithm to automatically adjust the exploration and exploitation efforts based on the search phase during operation, effectively avoiding premature convergence or low efficiency problems caused by fixed attenuation in the early stage or later stage.

3.2. Distance-fitness evaluation strategy

When the GSA algorithm selects individuals to guide the search, it usually only depends on the fitness value. If the algorithm selects individuals based only on fitness, the population may aggregate prematurely around a local optimum, lose diversity, and converge prematurely. Therefore, the distance-fitness evaluation strategy is proposed. By combining the fitness ranking and distance ranking of individuals, the distance fitness evaluation strategy can select the balanced individual who can not only use high-quality information but also bring exploration potential. Moreover, the original GSA did not use *gbest* and the historical location information found previously to guide the search process. For an individual x_i, its own role is also ignored in the calculation of gravity. Practice has proved that high-quality historical location information can guide the population to evolve in a more promising direction. Therefore, the historical location information is introduced into the distance-fitness evaluation strategy. The historical optimal location information of individuals is saved, and each individual can learn from other excellent particles to obtain additional guidance. The strategy is described as follows: in each generation, four individuals are randomly selected from the population to compare with the current individual, and the individual with the best historical location information will be the learning sample of the current individual. The formula is as follows:

$$pbest_{wi}(t) = \arg\min\left\{f(pbest_a(t)), f(pbest_b(t)), f(pbest_c(t)), f(pbest_d(t))\right\}, a \neq b \neq c \neq d \quad (11)$$

$$pbest_{ei}(t) = \begin{cases} pbest_{wi}(t), if\ f(pbest_{wi}(\mathrm{t})) < f(pbest_i(\mathrm{t})) \\ pbest_i(t), otherwise \end{cases} \quad (12)$$

Where, $f(\cdot)$ represents fitness function, $pbest_a(t)$, $pbest_b(t)$, $pbest_c(t)$ and $pbest_d(t)$ represent the historical optimal position of four randomly selected individuals. $pbest_{e,i}(t)$ represents the learning sample of the current individual. Calculate the distance from each particle *i* to the current fitness optimal particle:

$$diff_i(t) = \begin{cases} x_i(t) - pbest, if\, f(p\text{best}) < f(pbest_{ei}(t)) \\ x_i(t) - pbest_{ei}(t), otherwise \end{cases} \tag{13}$$

Where, $diff_i(t)$ is the distance from the individual to the historical optimal particle, and the optimal particle will be selected according to the fitness value of the individual. If the fitness value of the individual's historical optimal solution is better than the fitness value of the individual's learning sample, the original historical individual's optimal location information is retained. On the contrary, the original historical individual's optimal location information is replaced by the learning sample information. The Mahalanobis distance method will be used to calculate the distance between individuals. The covariance structure of the population will be considered in the Mahalanobis distance calculation method. The specific calculation formula is as follows:

$$Dis_i(t) = \sqrt{diff_i(t) \cdot \sum{}^{-1} diff_i(t)^T} \tag{14}$$

Where, $Dis(t)$ is the Mahalanobis distance, $\sum^{-1}$ is the inverse of the population covariance matrix, and $diff_i(t)^T$ is the transpose of the distance matrix. Using Mahalanobis distance in this strategy can take the correlation of data and the scale of different dimensions into account at the same time, and enable the algorithm to identify sparse regions more effectively and better adapt to the distribution of population. Individuals are ranked from large to small by distance. The greater the distance, the higher the exploration value. The farthest individual is ranked as 1, and the individual distance evaluation value is obtained $R_{d,i}$ .The optimal particle of fitness value is

ranked as 1, so the fitness evaluation value of each individual can be obtained $R_{f,i}$. The specific expressions of the two evaluation values are shown in equations (15) and (16).

$$R_{d,i} = rand_{d1} \tag{15}$$

$$R_{f,i} = rank_{f1} \tag{16}$$

$$S_{df,i} = R_{d,i} + R_{f,i} \tag{17}$$

Where, $S_{df,i}$ is the comprehensive evaluation value of the individual which includes the distance evaluation value and fitness evaluation value of the individual. The smaller the score, the better the balance between "good fitness" and "far from the current optimal" of the particle.The algorithm selects the individual with the lowest comprehensive evaluation value as the balanced guide. Through the comprehensive evaluation of individuals, the algorithm can not only rely on the global optimal solution to guide the update, but also rely on the balanced individual to update the algorithm. The new update strategy is described as follows:

$$v_i(t+1) = \begin{cases} rand \cdot v_i(t) + a_{0,i}(t) + rand \cdot (gbest - x_i(t)), if f(x_i(t)) < f(gbest_{df}) \\ rand \cdot v_i(t) + a_{0,i}(t) + rand \cdot (gbest_{df} - x_i(t)), otherwise \end{cases} \tag{18}$$

Where, *gbest* is the global optimal solution and $gbest_{df}$ is the balanced individual. In equation (18), when the fitness value of the balanced individual is better than the fitness value of the individual, the speed update of the algorithm will be calculated by the balanced individual. Otherwise, it will be guided by the global optimal solution. The distance-fitness evaluation strategy will redefine how to select *gbest*. Instead of just looking at fitness, it will comprehensively consider fitness and spatial distance, so as to select the particles with ‘the most guiding potential’ as the global guide, and prevent all particles from converging prematurely toward a potentially local optimum. The algorithm can also make better use of the excellent solution through such an update method. Therefore, the introduction of

distance-fitness evaluation strategy in the algorithm can significantly avoid premature convergence and maintain population diversity for a longer time. Although the exploration of the algorithm has increased, it can still efficiently locate the optimal region through intelligent balance, which makes the algorithm perform better on complex optimization problems.

3.3 The pseudocode of SDGSA

SDGSA first initializes the population and then calculates parameters using the self-adapting attenuation factor. As the iteration progresses, SDGSA will execute different speed-calculation methods. Based on the distance-fitness evaluation strategy, SDGSA uses different velocity-update methods during the iterative process. According to the distance evaluation, SDGSA can switch between speed-calculation methods to find the optimal solution. If the algorithm meets the stopping criteria, it outputs the optimal value. If the algorithm does not meet the stopping criteria, it will continue to run. The pseudocode of SDGSA is given in Algorithm 1.

Algorithm 1. The framework of SDGSA.

Initialize a population of particles with random solutions.
Initialize the velocities and positions randomly.
Evaluate the fitness values of agent x
While ($t <$ max _it)
    Produce the attenuation factor using Eq (9).
    Produce the gravity constant Eq (10).
    Find the individual best solution and the suboptimal solution in the individual history
    For $i = 1{:}N$
        Calculate the total force $F_i(t)$, the mass $m_i(t)$ and the acceleration $a_i(t)$
        Obtain the best historical location information using Eq (11) and (12).
        Calculate the Mahalanobis distance of an individual using Eq (13) and (14).
        Record the farthest particle ranking as 1 using Eq (15).

Calculate the individual fitness value, and rank the individual with the best fitness as 1. Record the ranking of fitness values using Eq (16).

Calculate the distance-fitness evaluation parameter using Eq (17).

Obtain the $gbest_{fd}$ with the minimum distance-fitness evaluation parameter.

Update the velocity of members using Eq (18).

Update the position of individual using Eq (8).

Calculate the fitness value of each particle.

Preserve the best solution.

End for

End while

Evaluate the fitness values

4. Experimental Results and Discussion

To verify the performance of SDGSA, two comparative experiments are carried out. The first experiment compares SDGSA with several GSA variants on fifty-eight test functions. The second experiment compares SDGSA with eleven metaheuristic algorithms on fifty-eight benchmark functions.

4.1. Experimental setup

The evaluation uses 58 functions, labeled F1-F58, drawn from the CEC2013 and CEC2017 suites. The first group contains 28 CEC2013 problems (F1-F28), and the second contains 30 CEC2017 problems (F29-F58). Using both suites broadens the evidence available for judging convergence reliability. Within CEC2013, F1-F5 are treated as unimodal, F6-F20 as multimodal, and F21-F28 as composition functions [18]. The CEC2017 subset contains three unimodal problems (F29-F31), seven simple multimodal problems (F32-F38), ten hybrid problems (F39-F48), and ten composition problems (F49-F58). F30 is omitted because its

results are unstable, particularly as dimensionality increases [19]. The shifted and rotated structures in CEC2017 also make this suite more demanding than elementary benchmarks .

4.2. Parameter analysis

The search effect of SDGSA will be affected by the size of parameter L. To study the influence of parameter L on the search effect of SDGSA, CEC2013 test functions are used for testing. These test functions include unimodal functions and multimodal functions. In this experiment, the range of parameter is set to be between 1 and 6. The population size of SDGSA is 50, the problem dimension is 30, and the maxFEs of the algorithm is set as 300,000. For each parameter L value and test problem, SDGSA is run independently 30 times. For parameter L, the experimental results are shown in table 1.

Table 1 Test function results with different L values

Fun	$L=1$	$L=2$	$L=3$	$L=4$	$L=5$	$L=6$
F1	7.11E–013	6.13E–013	2.96E–013	0.00E+000	0.00E+000	4.43E–013
F2	1.07E+007	1.21E+006	7.63E+005	2.45E+005	5.30E+005	6.83E+006
F3	1.12E+010	1.24E+010	1.07E+009	5.05E+006	1.94E+008	6.11E+009
F4	3.01E+004	3.70E+004	1.72E+003	3.97E+001	1.94E+002	2.38E+004
F5	4.42E+002	3.93E+002	1.14E–012	3.47E–012	7.16E–012	4.08E+002
F6	1.19E+002	1.24E+002	4.93E+001	7.23E+001	5.97E+001	8.98E+001
F7	1.53E+002	1.68E+002	9.58E+001	2.04E+001	9.19E+001	1.25E+002
F8	2.09E+001	2.09E+001	2.10E+001	2.10E+001	2.09E+001	2.09E+001
F9	2.71E+001	2.76E+001	2.61E+001	4.72E+001	2.44E+001	8.76E+001
F10	9.34E+001	1.41E+002	6.42E–002	5.43E–003	8.13E–002	2.50E+001
F11	4.17E+002	3.55E+002	2.52E+002	1.42E+002	2.55E+002	3.45E+002
F12	3.55E+002	3.58E+002	2.85E+002	1.30E+002	2.81E+002	3.68E+002
F13	4.61E+002	5.00E+002	3.62E+002	1.87E+002	3.65E+002	4.96E+002
F14	3.91E+003	3.90E+003	3.55E+003	3.18E+003	3.74E+003	5.94E+003
F15	4.22E+003	3.70E+003	3.47E+003	2.12E+003	3.54E+003	4.82E+003
F16	2.06E+000	1.90E+000	1.44E+000	2.16E–003	1.30E+000	2.08E+000
F17	4.37E+002	4.78E+002	2.81E+002	4.52E+001	1.96E+002	3.91E+002
F18	4.64E+002	4.66E+002	2.34E+002	5.89E+001	2.03E+002	3.51E+002
F19	4.63E+002	2.55E+002	8.70E+000	2.15E+000	8.45E+000	1.37E+002
F20	1.50E+001	1.50E+001	1.50E+001	1.50E+001	1.50E+001	1.50E+001

F21	3.72E+002	5.22E+002	3.11E+002	3.00E+002	3.11E+002	2.80E+002
F22	4.77E+003	4.90E+003	4.03E+003	3.38E+003	4.08E+003	6.50E+003
F23	4.64E+003	4.68E+003	4.44E+003	5.95E+003	4.19E+003	6.85E+003
F24	3.01E+002	3.06E+002	2.90E+002	2.47E+002	2.82E+002	3.96E+002
F25	3.22E+002	3.21E+002	3.07E+002	2.63E+002	3.07E+002	3.21E+002
F26	3.54E+002	3.45E+002	3.33E+002	2.15E+002	3.20E+002	3.38E+002
F27	1.09E+003	1.10E+003	1.26E+003	1.17E+003	1.04E+003	3.10E+003
F28	3.29E+003	3.78E+003	1.22E+003	2.66E+003	1.00E+003	3.20E+003
ARV	4.6250	4.8214	2.7679	1.9464	2.2679	4.5714
Rank	5	6	3	1	2	4

As shown in table 1, when the internal parameter L is set to 4, the SDGSA algorithm achieves high-precision solutions on 21 functions; Under other settings, its performance decreases. Obviously, the configuration of parameter L has a significant impact on the performance of the SDGSA algorithm. In addition, the Friedman test results indicate that under the configuration of L=4, the average ranking is always at the lowest level, indicating that the overall performance of the algorithm under this configuration is the best. Therefore, it is recommended to set the internal parameter L to 4 as the default configuration for this algorithm.

4.3. Comparison of the proposed SDGSA with GSA algorithms

Optimization accuracy is first examined against three gravity-search methods: GSA [3], ALGSA [6], and GGSA [16]. The evaluation draws on 58 functions from the CEC2013 and CEC2017 suites and considers D=30 and D=50. The population size N is fixed at 50. Within this comparison, 43 benchmark functions are used to characterize behavior at the two dimensionalities, and every run is limited to 300,000 function evaluations (maxFEs). Table 2 lists the parameter configuration for each optimizer; the numerical outcomes appear in Tables 3 and 4.

Table 2 Parameter settings of SDGSA and GSA algorithms.

Algorithm	Parameters
GSA	$G_0 = 100, a = 20$
ALGSA	$G_0 = 100, a = 20, p = 0.05$
GGSA	$G_0 = 100, a = 20, c_1(t) = 2 - 2t^3 / T^3, c_2(t) = 2t^3 / T^3$
SDGSA	$G_0 = 100, L = 4$

Table 3 Experimental results of benchmark functions (f1-f58) with *D*=30 dimensions using SDGSA and GSA algorithms.

Function	GSA		ALGSA		GGSA		SDGSA	
	mean	std	mean	std	mean	std	mean	std
F1	2.27E–013	1.13E–013	1.39E–009	3.81E–010	6.82E–013	8.62E–014	0.00E+000	0.00E+000
F2	1.96E+006	4.89E+005	3.53E+006	8.83E+005	5.91E+007	4.95E+005	2.45E+005	1.34E+005
F3	6.05E+007	4.17E+007	5.94E+007	7.58E+006	3.67E+008	2.49E+008	5.05E+006	5.45E+005
F4	6.90E+004	5.32E+003	6.62E+004	1.78E+004	6.69E+004	5.22E+003	3.97E+001	1.02E+002
F5	6.47E–012	2.49E–012	3.82E–006	1.91E–006	4.81E–012	2.21E–012	3.47E–012	2.27E–012
F6	3.56E+001	2.59E+001	6.64E+001	1.85E+001	3.80E+001	2.50E+001	7.23E+001	1.55E+001
F7	4.32E+001	9.30E+000	2.05E+001	4.01E+000	4.53E+001	1.04E+001	2.04E+001	6.76E+000
F8	2.10E+001	4.26E–002	2.11E+001	1.54E–001	2.11E+001	7.32E–002	2.10E+001	2.09E–002
F9	2.87E+001	3.94E+000	8.26E+000	1.84E+000	2.89E+001	3.51E+000	4.72E+001	3.14E+001
F10	8.55E–003	7.79E–003	2.71E–002	4.29E–003	1.16E–002	9.58E–003	5.43E–003	2.44E–003
F11	1.95E+002	2.53E+001	2.29E+002	6.96E+002	2.01E+002	2.59E+001	1.42E+002	1.82E+002
F12	2.13E+002	3.03E+001	2.98E+002	7.17E+001	2.23E+002	2.75E+001	1.30E+002	1.67E+001
F13	3.35E+002	4.16E+001	1.93E+002	4.81E+001	3.52E+002	3.83E+001	1.87E+002	3.47E+001
F14	3.38E+003	5.31E+002	3.20E+003	6.62E+002	3.34E+003	4.71E+002	3.18E+003	3.60E+002
F15	3.55E+003	4.44E+002	2.46E+003	4.69E+002	3.39E+003	4.65E+002	2.12E+003	3.69E+002
F16	3.47E–003	2.85E–003	2.72E–002	2.42E–002	4.36E–003	2.43E–003	2.16E–003	1.19E–003
F17	4.41E+001	3.11E+000	5.77E+001	8.52E+000	4.53E+001	4.16E+000	4.52E+001	5.20E+000
F18	4.54E+001	3.82E+000	6.31E+001	3.07E+000	4.34E+001	3.50E+000	5.89E+001	5.44E+001
F19	2.96E+000	4.76E–001	5.08E+000	5.18E–001	3.04E+000	6.98E–001	2.15E+000	2.47E+000
F20	1.50E+001	6.72E–013	1.50E+001	5.45E–009	1.58E+001	3.08E–001	1.50E+001	1.50E–010
F21	3.29E+002	5.84E+001	3.00E+002	3.69E–004	3.33E+002	6.18E+001	3.00E+002	3.00E–003
F22	5.69E+003	7.58E+002	3.89E+003	7.31E+002	5.64E+003	8.86E+002	3.38E+003	6.12E+002
F23	5.41E+003	3.98E+002	3.04E+003	1.83E+002	5.57E+003	3.70E+002	5.95E+003	4.56E+003
F24	2.71E+002	4.75E+001	2.60E+002	1.19E+002	2.71E+002	3.86E+001	2.47E+002	2.74E+002
F25	3.42E+002	3.12E+001	3.01E+002	1.87E+001	3.48E+002	3.15E+001	2.63E+002	3.06E+002
F26	3.28E+002	4.25E+001	2.27E+002	4.69E+001	3.29E+002	4.79E+001	2.15E+002	3.34E+001

F27	7.72E+002	9.71E+001	1.51E+003	1.20E+003	7.50E+002	1.27E+002	1.17E+003	9.04E+002
F28	3.23E+003	2.36E+002	4.62E+003	1.02E+001	3.23E+003	2.49E+002	2.66E+003	2.80E+003
F29	2.06E+003	1.57E+003	5.07E+002	3.43E+002	2.24E+003	1.64E+003	4.99E+002	2.98E+002
F31	7.72E+004	7.03E+003	9.59E+004	7.78E+003	6.50E+004	7.40E+003	3.00E+002	6.71E–011
F32	5.30E+002	1.15E+001	4.46E+002	1.33E+000	4.83E+002	2.26E+001	4.27E+002	2.14E+001
F33	7.14E+002	1.93E+001	7.22E+002	6.05E+001	7.08E+002	1.87E+001	6.63E+002	3.67E+001
F34	6.40E+002	5.22E+000	6.00E+002	1.09E–005	6.40E+002	5.29E+000	6.52E+002	3.07E+000
F35	7.69E+002	6.05E+001	7.48E+002	2.72E+001	8.48E+002	4.66E+001	7.85E+002	1.60E+001
F36	9.42E+002	1.41E+001	9.41E+002	2.52E+001	9.44E+002	2.00E+001	9.28E+002	2.77E+001
F37	1.35E+003	3.58E+002	9.00E+002	3.83E–003	1.38E+003	3.14E+002	3.73E+003	1.50E+003
F38	4.80E+003	4.30E+002	4.61E+003	6.07E+002	4.79E+003	5.02E+002	4.09E+003	4.66E+002
F39	1.21E+003	6.23E+001	1.21E+003	6.53E+001	1.38E+003	7.80E+001	1.20E+003	6.51E+001
F40	1.37E+006	2.51E+005	6.30E+004	5.06E+004	4.34E+005	2.82E+005	1.46E+004	3.52E+003
F41	2.84E+004	8.07E+003	4.54E+004	6.62E+003	2.45E+004	6.33E+003	1.60E+004	8.50E+003
F42	8.37E+004	3.64E+004	3.51E+003	1.42E+003	1.10E+005	3.33E+004	2.02E+003	1.27E+003
F43	6.12E+003	1.94E+003	2.16E+003	2.27E+002	4.19E+003	1.55E+003	3.91E+003	1.52E+004
F44	3.21E+003	3.24E+002	3.30E+003	2.00E+002	3.12E+003	3.10E+002	3.12E+003	3.05E+002
F45	2.79E+003	2.46E+002	2.88E+003	2.11E+002	2.73E+003	1.94E+002	2.43E+003	1.79E+002
F46	2.37E+005	9.70E+004	1.82E+005	8.09E+004	2.30E+005	7.88E+004	4.67E+004	1.42E+004
F47	5.69E+003	1.72E+003	1.82E+004	8.30E+003	5.22E+003	1.28E+003	6.75E+003	3.80E+003
F48	3.06E+003	2.27E+002	2.70E+003	1.63E+002	3.07E+003	2.34E+002	2.63E+003	1.29E+002
F49	2.51E+003	6.46E+001	2.32E+003	1.08E+001	2.52E+003	1.89E+001	2.53E+003	4.25E+001
F50	4.89E+003	2.31E+003	2.47E+003	6.06E+001	4.42E+003	2.48E+003	2.30E+003	2.45E+001
F51	3.39E+003	1.23E+002	3.69E+003	1.24E+002	3.38E+003	1.31E+002	3.19E+003	1.09E+002
F52	3.14E+003	4.95E+001	3.82E+003	1.55E+001	3.14E+003	5.39E+001	3.05E+003	1.10E+002
F53	2.92E+003	1.52E+001	2.89E+003	3.30E+000	2.90E+003	1.45E+001	2.89E+003	2.34E+001
F54	4.00E+003	1.73E+003	3.93E+003	6.28E+002	4.26E+003	1.78E+003	6.56E+003	2.52E+003
F55	3.83E+003	2.27E+002	3.29E+003	3.28E+001	3.85E+003	2.73E+002	3.23E+003	2.50E+001
F56	3.21E+003	4.31E+001	3.20E+003	9.77E+001	3.18E+003	2.33E+001	3.16E+003	1.91E+001
F57	4.46E+003	2.12E+002	3.47E+003	7.21E+002	4.38E+003	2.75E+002	2.14E+003	1.48E+002
F58	3.72E+004	8.68E+003	1.57E+004	3.25E+003	3.37E+004	8.19E+003	1.16E+004	1.01E+004
+/≈/–	53/2/2		47/3/7		53/1/3			
AVR	2.8158		2.5702		2.9737		1.6404	

As shown in table 3, SDGSA obtained the best results in 43 of the 58 test cases (i.e., F1-F5, F7, F8, F10-F16, F19-F22, F24-F26, F28-F33, F36, F38-F42, F44-F46, F48, F50-F53 and F55-F58). Meanwhile, SDGSA achieved suboptimal results on F17 and F43. ALGSA performs excellently in F9, F20, F21, F23, F13, F34, F35, F37, F43, F49, F53, and F54. It is worth noting that GSA only outperforms other competitors on F6, F8, F17, F20, and F44. GGSA performs

better than other algorithms on F18, F27, F44, and F47. In addition, the GSA, ALGSA, and SDGSA algorithms yield completely consistent results on F20.

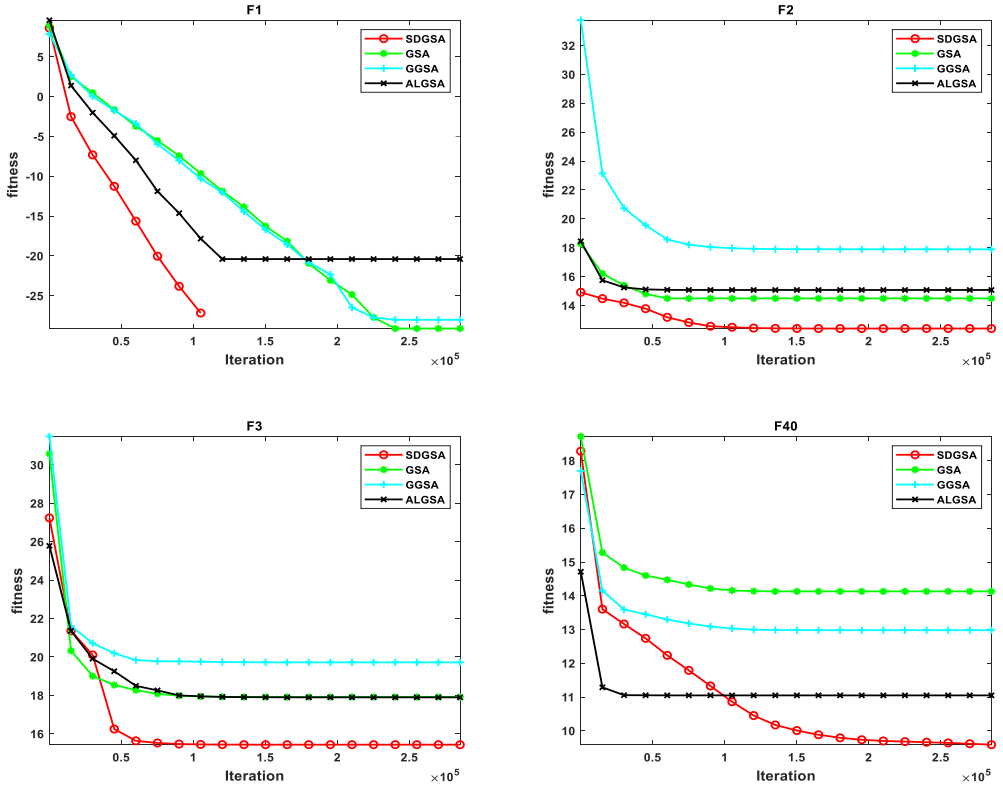


Figure 1 The convergence curves of SDGSA and GSA algorithms on some test functions.

Figure 1 shows the convergence behavior of SDGSA and GSA algorithms on F1, F2, F3 and f40 with 30 dimensions. According to figure 1, SDGSA shows a different convergence characteristic. SDGSA converges consistently during the first half of the search process and finally obtains the best solution in a later stage. Therefore, this result verifies that SDGSA achieves higher convergence accuracy.

Table 4 Experimental results of benchmark functions (f1-f58) with D=50 dimensions using SDGSA and GSA algorithms.

Function	GSA		ALGSA		GGSA		SDGSA	
	mean	std	mean	std	mean	std	mean	std
F1	2.27E–013	0.00E+000	4.69E–007	1.13E–006	2.35E–013	4.15E–014	0.00E+000	0.00E+000

F2	2.46E+006	5.54E+005	1.35E+007	4.16E+006	2.24E+006	6.09E+005	2.04E+006	1.20E+006
F3	2.18E+009	1.26E+009	1.21E+008	4.06E+007	2.46E+009	1.28E+009	1.48E+007	1.76E+006
F4	9.19E+004	6.51E+003	8.62E+004	2.51E+004	8.96E+004	5.38E+003	9.01E+003	3.96E+003
F5	6.09E–012	1.78E–012	1.52E–007	1.24E–005	5.57E–012	1.94E–012	1.36E–011	1.04E–011
F6	8.37E+001	2.44E+001	1.46E+002	6.07E–001	8.36E+001	2.05E+001	4.97E+001	2.95E+001
F7	6.11E+001	6.20E+000	2.23E+002	2.42E+000	5.96E+001	6.39E+000	1.20E+002	3.69E+001
F8	2.11E+001	4.12E–002	3.21E+002	8.72E–002	2.11E+001	5.32E–002	2.10E+001	6.65E–002
F9	4.58E+001	4.81E+000	4.24E+002	5.60E+001	4.37E+001	4.67E+000	2.59E+001	3.26E+000
F10	1.73E–001	1.13E–001	5.01E+002	6.84E–001	1.76E–001	9.69E–002	2.89E–001	2.94E–001
F11	4.11E+002	3.78E+001	6.55E+002	1.00E+001	4.00E+002	3.78E+001	2.61E+002	9.85E+001
F12	6.59E+002	6.62E+001	7.42E+002	9.24E+000	6.93E+002	5.93E+001	2.46E+002	6.68E+000
F13	7.91E+002	8.70E+001	9.59E+002	2.96E+001	7.93E+002	7.45E+001	3.78E+002	9.18E+001
F14	6.24E+003	5.69E+002	6.32E+003	9.98E+002	6.14E+003	7.11E+002	3.99E+003	5.79E+002
F15	8.16E+003	7.24E+002	7.29E+003	6.46E+002	8.01E+003	5.20E+002	4.05E+003	8.59E+002
F16	4.87E–003	1.76E–003	1.20E+003	2.31E–003	5.65E–003	2.02E–003	2.03E+000	2.45E–001
F17	1.28E+002	2.54E+001	1.41E+003	1.09E+001	1.36E+002	1.85E+001	3.03E+002	3.55E+001
F18	1.13E+002	1.31E+001	1.50E+003	2.00E+001	1.13E+002	1.87E+001	3.99E+002	1.67E+002
F19	6.49E+000	1.06E+000	1.51E+003	1.45E+000	6.28E+000	1.46E+000	1.22E+001	1.47E+000
F20	2.45E+001	3.35E–001	1.62E+003	2.29E+000	2.45E+001	3.07E–001	1.50E+001	4.41E–011
F21	9.51E+002	1.42E+002	2.54E+003	1.65E+002	1.01E+003	1.42E+002	3.72E+002	8.29E+001
F22	1.19E+004	5.13E+002	7.50E+003	1.37E+003	1.21E+004	4.81E+002	4.46E+003	7.49E+002
F23	1.10E+004	4.35E+002	7.44E+003	1.34E+003	1.11E+004	4.95E+002	4.71E+003	7.30E+002
F24	3.22E+002	1.58E+001	2.21E+003	1.71E+001	3.27E+002	1.72E+001	2.88E+002	9.73E+000
F25	5.96E+002	2.16E+001	2.47E+003	5.04E+000	5.79E+002	2.72E+001	3.08E+002	8.32E+000
F26	4.05E+002	8.56E+001	2.54E+003	3.18E+000	3.54E+002	1.03E+002	2.15E+002	2.78E+000
F27	1.72E+003	1.46E+002	3.26E+003	1.19E+002	1.70E+003	1.67E+002	9.54E+002	6.69E+001
F28	7.21E+003	4.43E+002	5.93E+003	1.80E+003	7.12E+003	4.78E+002	3.24E+003	6.55E+002
F29	1.96E+003	1.19E+003	2.42E+004	9.31E+003	2.24E+003	1.64E+003	1.80E+003	1.52E+003
F30	/	/	/	/	/	/	/	/
F31	1.72E+005	1.48E+004	2.08E+005	2.15E+004	6.50E+004	7.40E+003	3.13E+002	2.18E+000
F32	5.81E+002	6.47E+001	5.60E+002	4.12E+001	4.83E+002	2.26E+001	5.94E+002	3.38E+001
F33	8.28E+002	2.48E+001	5.66E+002	9.97E+000	7.08E+002	1.87E+001	8.43E+002	5.96E+001
F34	6.53E+002	4.30E+000	6.00E+002	3.81E–002	6.40E+002	5.29E+000	6.60E+002	1.81E+000
F35	8.83E+002	3.39E+001	7.90E+002	1.08E+001	7.98E+002	4.66E+000	7.46E+002	2.38E+000
F36	1.15E+003	2.63E+001	8.53E+002	1.94E+001	9.44E+002	2.00E+001	8.47E+002	1.64E+001
F37	7.93E+003	9.61E+002	9.00E+002	7.43E–001	1.38E+003	3.14E+002	9.00E+002	8.72E–001
F38	7.63E+003	6.96E+002	4.03E+003	7.75E+002	4.79E+003	5.02E+002	3.81E+003	2.84E+002
F39	1.49E+003	1.01E+002	3.27E+003	7.16E+002	1.18E+003	1.80E+001	1.00E+003	8.78E+000
F40	1.64E+006	6.18E+005	5.02E+005	2.55E+005	6.54E+005	2.82E+005	3.88E+005	1.79E+005
F41	2.54E+004	5.27E+003	1.42E+004	1.22E+003	2.45E+004	6.33E+003	2.52E+003	7.56E+002
F42	2.11E+005	2.09E+005	1.52E+003	4.40E+001	5.39E+004	3.33E+004	2.36E+004	2.16E+004
F43	1.42E+004	3.60E+003	6.43E+003	1.12E+003	4.19E+003	1.55E+003	2.32E+003	2.44E+002
F44	3.47E+003	3.62E+002	2.74E+003	3.05E+002	3.12E+003	3.10E+002	1.62E+003	2.68E+002
F45	3.53E+003	3.23E+002	1.57E+006	1.55E+006	3.73E+003	1.94E+002	3.01E+003	2.26E+002

F46	1.14E+006	8.55E+005	1.50E+004	3.84E+003	1.45E+005	7.88E+004	7.41E+004	4.26E+004
F47	1.73E+004	4.55E+003	8.38E+003	2.10E+003	5.22E+003	1.28E+003	1.66E+004	6.45E+003
F48	3.59E+003	3.82E+002	3.49E+003	2.35E+002	3.37E+003	2.34E+002	3.20E+003	1.59E+002
F49	2.88E+003	3.31E+001	2.81E+003	1.84E+001	2.97E+003	1.89E+001	2.75E+003	8.36E+001
F50	1.08E+004	7.45E+002	2.30E+003	2.29E–005	4.42E+003	2.48E+003	2.62E+003	8.62E+002
F51	4.16E+003	1.93E+002	2.79E+003	3.81E+001	3.38E+003	1.31E+002	3.86E+003	2.37E+002
F52	3.68E+003	7.84E+001	3.00E+003	2.04E+001	3.14E+003	5.39E+001	3.00E+003	2.93E+001
F53	3.22E+003	7.56E+001	3.02E+003	1.89E+001	3.97E+003	1.45E+001	3.01E+003	1.11E+001
F54	6.47E+003	2.99E+003	4.96E+003	9.39E+001	4.26E+003	1.78E+003	4.84E+003	3.36E+003
F55	6.12E+003	4.14E+002	4.95E+003	2.84E+001	4.88E+003	2.73E+002	4.83E+003	1.15E+003
F56	3.48E+003	8.79E+001	3.39E+003	7.39E+000	3.18E+003	2.33E+001	3.41E+003	2.43E+001
F57	5.33E+003	3.19E+002	4.22E+003	1.43E+002	4.38E+003	2.75E+002	4.22E+003	1.74E+002
F58	2.81E+007	8.47E+006	6.83E+006	2.07E+005	3.37E+007	8.19E+006	1.69E+006	4.91E+005
+/≈/–	53/1/3		48/2/7		48/1/8			
AVR	3.0877		2.8421		2.4035		1.6667	

As shown in Table 4, SDGSA is also competitive in handling 50-dimensional functions. Specifically, SDGSA outperforms other algorithms on the 37 functions F1-F4, F6, F8, F9, F11-F15, F20-F29, F31, F35, F36, F38-F41, F43-F45, F48, F49, F53, F55, and F58. The difference in effectiveness between SDGSA and ALGSA is relatively small on F37, F52, and F57. ALGSA performs well on 9 functions including F33, F34, F37, F42, F46, F50-F52, and F57, but has poor performance in solving F1, F8, F9, F16, and F45. GGSA has achieved satisfactory solutions on functions F5, F7, F18, F19, F32, F47, F54, and F56. For the basic GSA algorithm, it achieved the lowest average on functions F10, F16, and F17, but performed the worst on 26 functions including F4, F15, F14, F25, F26, F28, F35-F38, F40-F44, F46-F48, and F50-F57. The proposed SDGSA significantly outperforms the other methods, while GSA performs the worst. In terms of 50 dimensional comparison, the Friedman test results also indicate that SDGSA ranks first with the lowest value of 1.6667. Therefore, compared with three similar methods, the proposed SDGSA method has better overall performance.

4.4. Comparison of the proposed SDGSA with GWO, DBO, SCA, AEFA, ASO, PSO, MRFO, ISA, FDA, ABC and SMA.

A second experiment places SDGSA against eleven non-GSA metaheuristics: GWO [20], DBO [21], SCA [22], AEFA [23], ASO [24], PSO [25], MRFO [26], ISA [27], FDA [28], ABC [29], and SMA [30]. For every benchmark, each method is executed independently 30 times. The settings in Table 5 were determined experimentally through trial-and-error tuning. The evaluation covers all 58 functions at D=30 and D=50, with a budget of 300,000 function evaluations per run. Overall differences are examined using the Friedman procedure, and pairwise significance is assessed by the Wilcoxon rank-sum test. Tables 6 and 7 report the 30-dimensional analysis, while Tables 8 and 9 give the corresponding results for D=50. Function-level statistics are available in Appendix Tables A1-A4.

Table 5 Parameter settings of SDGSA and other algorithms

Algorithm	parameters
SDGSA	N=30, L=4
GWO	N=30, a linearly decreases from 2 to 0
DBO	N=30, number of ball-rolling dung beetle:0.2·N
SCA	N=30, a linearly decreases from 2 to 0
AEFA	N=50, $K_0 = 500, a = 30$
ASO	N=50, $\beta = 0.2, \alpha = 30$
PSO	N=40, $c_1 = c_2 = 2$, ω linearly decreases from 0.9 to 0.4
MRFO	N=30, S= 2
ISA	N=50, a linearly increases from 0 to 1
FDA	N=50, $\beta = 1$
ABC	N=50, food sources:N/2, limit:N/2·D
SMA	N=30, z=0.03

Table 6 Experimental results yielded by 11 algorithms under Friedman test (D=30)

Final ranking	Algorithm	AVR
1	SDGSA	4.6140
2	PSO	4.9667

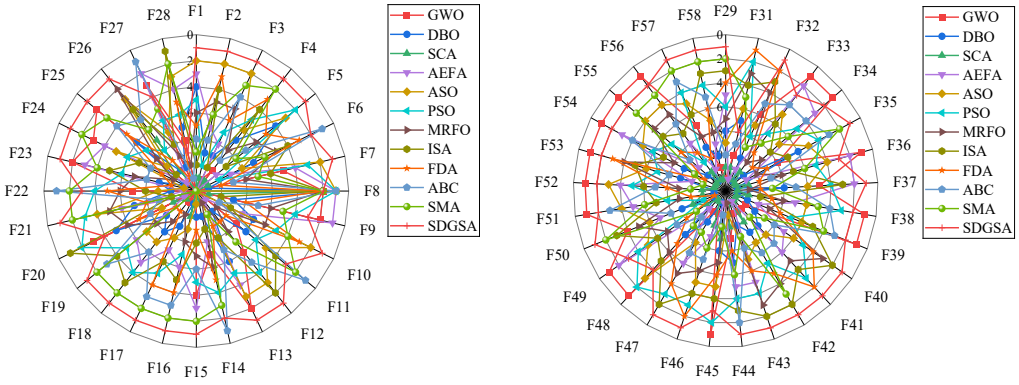
3	ISA	5.4561
4	ABC	5.4737
5	SMA	5.5702
6	ASO	5.7386
7	GWO	6.2719
8	FDA	6.4000
9	MRFO	6.7421
10	AEFA	7.5404
11	DBO	8.1895
12	SCA	11.0368

Table 7 Experimental results yielded by comparative algorithms under Wilcoxon rank sum test (*D*=30)

Algorithm	+	≈	–
SDGSA vs. GWO	38	2	17
SDGSA vs. DBO	42	4	11
SDGSA vs. SCA	50	2	5
SDGSA vs. AEFA	42	1	14
SDGSA vs. ASO	41	3	13
SDGSA vs. PSO	39	3	15
SDGSA vs. MRFO	40	2	15
SDGSA vs. ISA	39	3	15
SDGSA vs. FDA	40	4	13
SDGSA vs. ABC	39	2	16
SDGSA vs. SMA	44	2	11

According to the average ranking values in table 6, SDGSA ranks first with the lowest value of 4.6140, indicating the best overall performance. Meanwhile, SCA produced the highest average ranking value of 11.0368, indicating its worst performance in solving these functions. To further investigate whether there is a significant difference between SDGSA and other algorithms, the Wilcoxon rank-sum test was performed, and the results are shown in table 7. Specifically, SDGSA significantly outperforms its corresponding opponents on at least 40 functions and is inferior to them on a maximum of 16 functions. Overall, compared with the eleven advanced non-GSA algorithms, the proposed SDGSA is more competitive.

Table 7 shows the experimental results of the Wilcoxon rank sum test. Among them, "+", "=", and "-" respectively indicate that SDGSA performs significantly better than, comparable to, or inferior to its competitors on various functions. Obviously, SDGSA outperforms other algorithms on at least 38 functions, but performs poorly on up to 17 functions. In summary, among these 11 methods, SDGSA achieved the best convergence performance.



(a) CEC2013 test functions radar chart (b) CEC2017 test functions radar chart

Figure 2 Radar plots of SDGSA and other algorithms under 30 dimensional test functions

Figure 2 shows the radar chart sorted based on the average value in table 6. Obviously, compared to other optimization algorithms, SDGSA has produced more promising results in solving complex benchmark functions for CEC2013 and CEC2017. Therefore, the SDGSA algorithm is a highly competitive optimization method.

Table 8 Experimental results yielded by 11 algorithms under Friedman test (D=50)

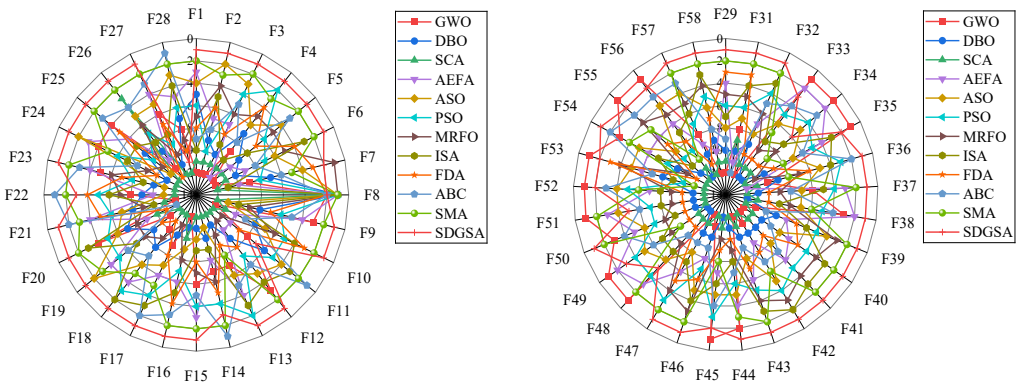
Final ranking	Algorithm	AVR
1	SDGSA	3.0351
2	PSO	5.2368
3	SMA	5.4123
4	ISA	5.5088
5	AEFA	5.9035
6	ASO	6.1667
7	ABC	6.1930
8	GWO	6.6930

9	MRFO	6.7368
10	FDA	6.8684
11	DBO	8.7982
12	SCA	11.4474

Table 9 Experimental results yielded by comparative algorithms under Wilcoxon rank sum test (*D*=50)

Algorithm	+	≈	–
SDGSA vs. GWO	47	2	8
SDGSA vs. DBO	48	3	6
SDGSA vs. SCA	53	3	1
SDGSA vs. AEFA	47	3	7
SDGSA vs. ASO	44	3	10
SDGSA vs. PSO	40	5	12
SDGSA vs. MRFO	47	3	7
SDGSA vs. ISA	44	3	10
SDGSA vs. FDA	47	3	7
SDGSA vs. ABC	42	4	11
SDGSA vs. SMA	40	5	12

As the dimensionality of the problem increases, the quality of the algorithm's solution on some complex functions begins to decline. SDGSA achieved the lowest average ranking (3.0351), followed closely by PSO and SMA; SCA achieved the highest average ranking (11.4474). Therefore, among the 11 compared algorithms, the proposed SDGSA performs the best, while SCA performs the worst. In addition, the Wilcoxon rank sum test was used to further analyze the performance differences between other compared algorithms. Table 9 shows the experimental results of the Wilcoxon rank sum test. Obviously, SDGSA outperforms other algorithms on at least 40 functions, but performs poorly on up to 12 functions. In summary, among these 11 methods, SDGSA achieved the best convergence performance.



(a) CEC2013 test functions radar chart (b) CEC2017 test functions radar chart

Figure 3 Radar plots of SDGSA and other algorithms under 50 dimensional test functions

Figure 3 shows the radar images of SDGSA and other algorithms for 50-dimensional test functions. The grid markings in the figure indicate the fitness ranking of the algorithm under this test function. From figure 3, it can be seen that SDGSA performs better than other algorithms in the above-mentioned problems.

4.5. Component analysis

As mentioned earlier, to improve performance, SDGSA introduces two core components: an adaptive attenuation factor and a distance-fitness evaluation strategy. To investigate the impact and effectiveness of various components on the performance of SDGSA, multiple improved versions of SDGSA are compared with GSA and the standard version of SDGSA. The experiments use 58 benchmark functions in 30 dimensions. In the experiment, the parameter settings are the same as in table 4. The specific improved version description is as follows:

- P1: SDGSA without distance-fitness evaluation strategy.
- P2: SDGSA with original attenuation coefficient and distance-fitness evaluation strategy.

Table 10 The differences between the considered variants of SDGSA and the original GSA.

Algorithm	adaptive attenuation factor	Distance-fitness evaluation strategy	Mean rank
GSA			4.00
P1	√		2.73
P2		√	2.13
SDGSA	√	√	1.16

The mean ranks in Table 10 order the four variants as SDGSA, P2, P1, and GSA. SDGSA obtains the best value (1.16), whereas the baseline GSA receives the worst (4.00). Three observations follow from this ablation study. First, both P1 and P2 improve convergence relative to GSA, showing that either proposed component is useful when introduced separately; the distance-evaluation component produces the larger individual gain. Second, the P1-versus-P2 result shows that the mechanisms contribute differently and supports their coordinated use. Finally, the complete SDGSA achieves the leading rank, confirming that their joint configuration provides the most effective of the tested designs.

4.6. Discussion of the comparative results

Tests on 58 problems at 30 and 50 dimensions provide an overall view of SDGSA's behavior. In solution accuracy, it ranks ahead of the original GSA, two enhanced GSA variants, and 11 established optimizers; both nonparametric analyses also identify a significant advantage over the competing methods. The SDGSA algorithm introduces an adaptive decay factor to adjust the decay rate of the gravity constant, thereby better balancing the trade-off between exploration and exploitation. Secondly, the SDGSA algorithm introduces a distance- fitness value evaluation strategy that considers both fitness value and particle spacing when evaluating the quality of the solution. Under this strategy, SDGSA can

choose a ‘Balanced Guide’ that can utilize high-quality information while maintaining exploration potential. SDGSA can choose to use ‘Balanced Guide’ or global optimal solutions for updates, rather than relying solely on the global optimal solution as the update guide. The distance-fitness evaluation strategy can effectively improve the algorithm’s tendency to fall into local optima and maintain algorithm diversity. In summary, SDGSA has excellent search performance and is very suitable for solving complex optimization problems.

5. UAV path planning problem

In this section, the SDGSA algorithm is applied to solve the path planning problem of unmanned aerial vehicles in complex environments. The drone path planning problem is essentially an optimization problem: its goal is to generate a smooth, minimum-cost path from the starting point to the target while avoiding obstacles and threat zones [31].

An environmental model is essential for evaluating whether UAVs can complete their assigned tasks successfully. The first step is to represent the obstacles in the planning space [32]. The function expression for simulating geomorphic features is:

$$z = (x, y) = \sin(y + a) + b\sin(x) + c\cos(d\sqrt{x^2 + y^2}) + e\cos(y) + f\sin(f\sqrt{x^2 + y^2}) + g\cos(y) \quad (19)$$

Among them, (x, y) is the coordinate of a point projected onto the horizontal plane on the terrain, and z is the height of the corresponding point coordinate. In Equation (19), a, b, c, d, e, f, and g are constant coefficients. Mountain-peak models need to be overlaid on the benchmark terrain.

$$h(x, y) = \sum_i h_i \exp[-\frac{(x - x_{oi})^2}{a_i^2} - \frac{(y - y_{oi})^2}{b_i}] + h_o \quad (20)$$

In equation (20), h_o and h_i respectively represent the reference terrain and the height of the *i*-th mountain peak, (x_{oi}, y_{oi}) represents the center coordinate position of the *i*-th mountain peak, and a_i and b_i are the slopes of the *i*-th mountain peak along the *x*-axis and *y*-axis directions, respectively. Route feasibility also depends on avoiding regions that endanger flight. These regions are treated as forbidden threat zones and must not be crossed by a planned UAV trajectory. For a tractable model, each threat zone is represented by a cylinder of radius *r*; changing *r* changes the area excluded from the route. Based on the actual situation, this article adopts a relatively complex trajectory evaluation function for unmanned aerial vehicle path planning. The path length is defined as the distance traveled by the drone from the starting point to the ending point. A complete flight path contains n nodes, and the trajectory must satisfy the following conditions:

$$L_p = \sum_{i=1}^{n-1} \| (x_{i+1}, y_{i+1}, z_{i+1}) - (x_i, y_i, z_i) \|_2 \tag{21}$$

Where represents the Euclidean distance between the *i*-th waypoint and the (*i*+1)-th waypoint. When the condition in Eq. (21) is satisfied, the UAV has encountered an obstacle or entered a threat zone. The altitude of a drone during flight will determine its safety and economy, so a stable flight altitude is crucial. The model function of drone flight altitude is as follows:

$$H_h = \sqrt{\frac{1}{n}\sum_{i=0}^{n-1}(z(i) - \frac{1}{n}\sum_{i=0}^{n-1} z(i))^2} \tag{22}$$

The operability of drones is also limited by their turning cost function. The turning angle of the drone during flight should not exceed its preset maximum turning angle, as the size of the turning angle will affect its flight stability. In this article, the maximum turning angle of the

drone is set as φ, and a_i is the vector of the i-th segment of the route. The specific expression is as follows:

$$F_t = \sum_{i=1}^{n} (\cos(\varphi - \frac{a_i \cdot a_{i+1}}{|a_i| \cdot |a_{i+1}|})) \tag{23}$$

Among them, $|a|$ represents the length of vector a. The cost function for unmanned aerial vehicle trajectory planning has been established based on the above constraints, and the specific expression is shown below:

$$F_c = w_1 \cdot L_p + w_2 \cdot H_h + w_3 \cdot F_t \tag{24}$$

where F_c is the total cost function, and the parameters w_i (i = 1, 2, 3) are the weights assigned to the individual cost terms and satisfy the following conditions:

$$\sum_{i=1}^{3} w_i = 1, (w_i \geq 0) \tag{25}$$

Based on the above drone path planning model, this paper constructs two different terrain scenarios.

Scenario 1: For a map of size 200×200, the threat-zone radius is set to 30, the height is set to 50, and the number of route nodes is set to 5. The shape of the mountain peak is relatively regular, and its height gradually increases from the starting point to the ending point. The specific map parameters are shown in table 11.

Table 11 The mountain information in the Scenario 1

	Center coordinates of the mountain peak	Peak height	Slope in the x-direction of the mountain peak	Slope in the y-direction of the mountain peak
Peak 1	[60, 60]	30	20	20
Peak 2	[100, 100]	60	30	30
Peak 3	[150, 150]	80	20	20

Scenario 2: In the threat area with a map size of 200×200, the radius is set to 40 and the height is set to 60, the number of route nodes is set to 5. The terrain is irregular, and the

mountain height fluctuates from the starting point to the endpoint. The threat zones also occupy a larger portion of the map. The specific map parameters are shown in table 12.

Table 12 The mountain information in the Scenario 2

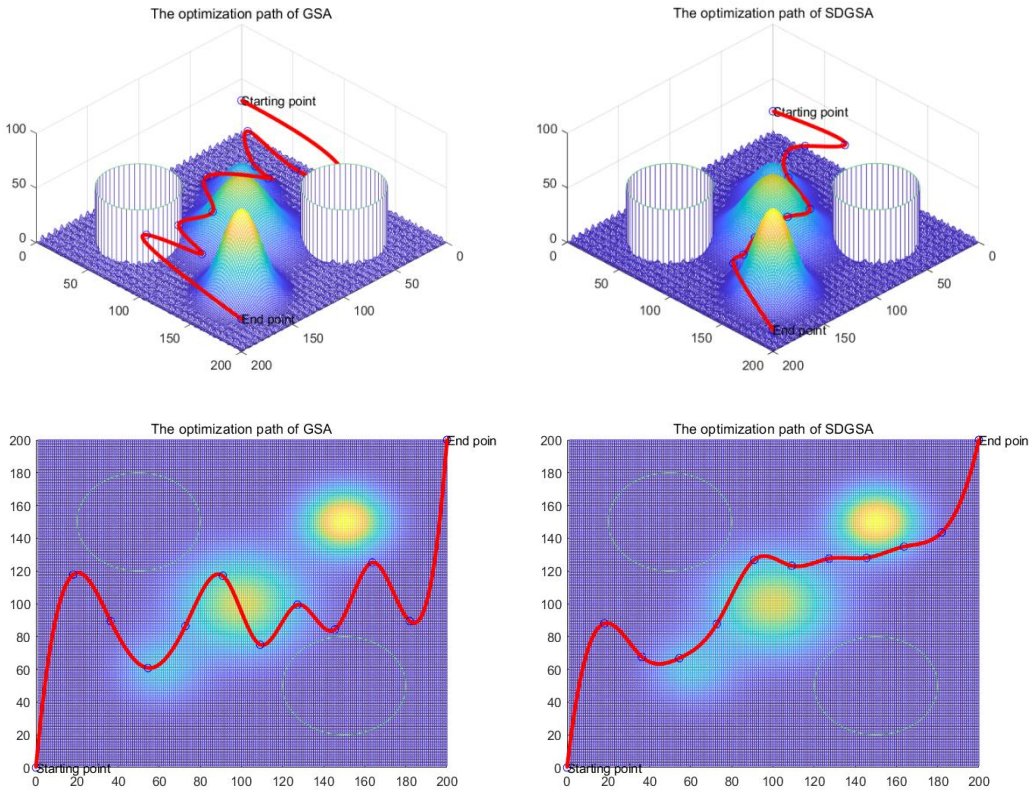
	Center coordinates of the mountain peak	Peak height	Slope in the x-direction of the mountain peak	Slope in the y-direction of the mountain peak
Peak 1	[40, 40]	50	20	20
Peak 2	[110, 110]	60	30	30
Peak 3	[160, 160]	50	80	30

5.1 Trajectory planning

The classic GSA is selected for comparison with the SDGSA. In the simulation experiment, both algorithms use 50 sample points as the population size. Each algorithm is run independently 30 times, with 100 iterations, and the remaining control parameters are set as listed in table 2. In addition, the average fitness value (AFV), average path length (APL) and average execution time (AET) generated by drones have been adopted as evaluation indicators. The simulation results are detailed in tables 13 and 14. Figures 4 and 6 respectively show the example paths generated by GSA and SDGSA in Scenario 1 and Scenario 2. Figures 5 and 7 show the convergence iteration curves of GSA and SDGSA in Scenario 1 and Scenario 2 , respectively.

Table 13 The simulation results of SDGSA and the original GSA in the Scenario 1

	GSA	SDGSA
Average fitness value	764.3194	162.6197
Average path length	613.11	374.62
Average execution time	203.82	91.43



(a) GSA **(b)** SDGSA

Figure 4 Optimization path of GSA and SDGSA in the Scenario 1

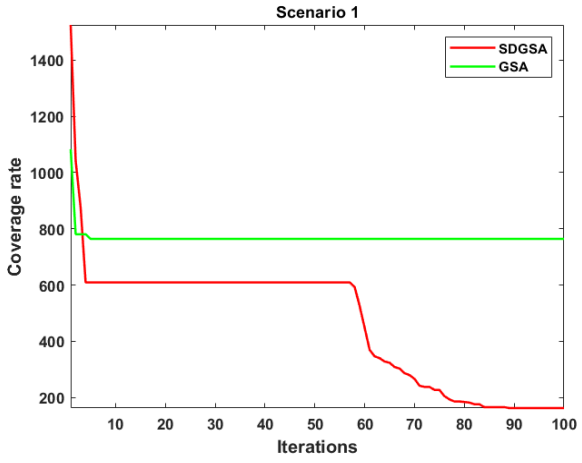


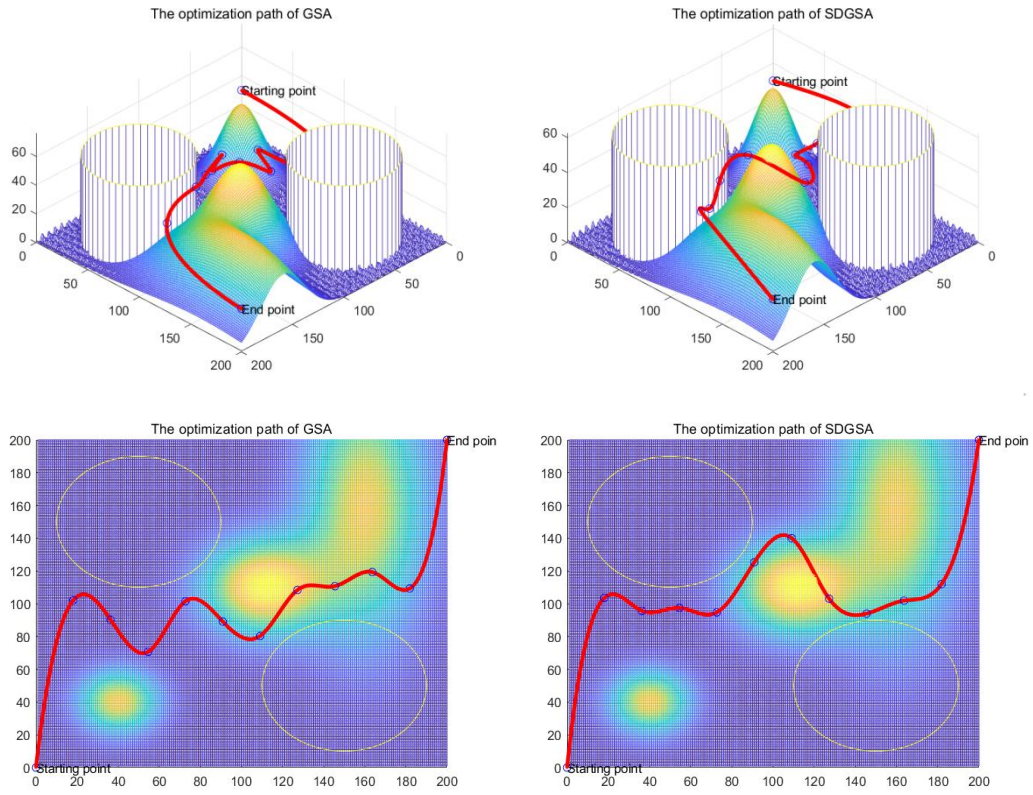
Figure 5 Curve of GSA and SDGSA in the Scenario 1

As shown in table 13, compared with GSA, SDGSA reduces the average path length, average execution time, and average fitness value by 38.9%, 55.1%, and 78.7%, respectively, indicating that the UAVs can reach their target positions along shorter paths. Meanwhile, the

shorter time required for SDGSA to complete path planning indicates its higher search efficiency. From figure 4, it can be seen that the path planned by SDGSA is superior to the path planned by GSA. From figure 5, it can be seen that the convergence accuracy of SDGSA is better than that of GSA, indicating that SDGSA has better performance in solving the problem in scenario 1.

Table 14 The simulation results of SDGSA and the original GSA in the Scenario 2

	GSA	SDGSA
Average fitness value	1206.0382	479.6576
Average path length	689.62	419.10
Average execution time	305.94	201.38



(a) GSA **(b)** SDGSA

Figure 6 Optimization path of GSA and SDGSA in the Scenario 2

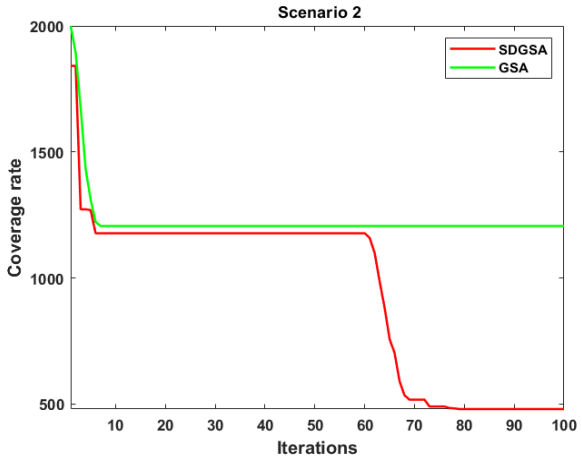


Figure 7 Curve of GSA and SDGSA in the Scenario 2

Scenario 2 increases both terrain irregularity and the extent of the threat regions, making the routing task more demanding. Even under these conditions, Table 14 reports smaller values for SDGSA than for GSA on all three measures. Relative to GSA, SDGSA reduces average path length by 39.2%, average execution time by 34.2%, and average fitness value by 60.2%. Figure 6 shows that the routes produced by both algorithms become more winding as environmental complexity rises, but the SDGSA route remains shorter and more favorable. Its lower fitness value and shorter computation time indicate that it searches the feasible space more effectively. These results support the use of SDGSA as a practical optimizer for difficult path-planning and related complex problems.

6. Conclusion

In this paper, a gravity search algorithm with a self-adaptive attenuation factor and a distance-fitness evaluation strategy (SDGSA) is proposed to improve the performance of the conventional GSA. Because the conventional GSA is prone to becoming trapped in local optima and has limited search capability, SDGSA incorporates a self-adaptive attenuation

factor into the parameter-update mechanism. This factor enables broad exploration during the early stages of the search and finer local exploitation during later stages, thereby improving both solution diversity and accuracy. SDGSA also employs a distance-fitness evaluation strategy to preserve population diversity and reduce the likelihood of premature convergence. Two sets of comparative experiments evaluate SDGSA against several GSA variants and eleven metaheuristic algorithms on the CEC2013 and CEC2017 benchmark functions. The results show that SDGSA outperforms the comparison algorithms. Its practical applicability is further evaluated on a UAV path-planning problem, where it performs more effectively than the conventional GSA. Overall, SDGSA is an effective and competitive optimization algorithm.

Acknowledgments

This work was supported by the 2025 Guangxi University Research Foundation for Enhancing the Basic Research Capabilities of Young and Middle-Aged Faculty (Grant No. 2025KY1074).

Conflicts of interest

The authors declare that there is no conflict of interest regarding the publication of this paper.

Data availability statement

All data that support the findings of this study are included within the article (and any supplementary files).

Appendix

See Tables A1-A4.

Table A1

Results of SDGSA with GWO, DBO, SCA, AEFA, ASO and PSO for the 30-dimensional CEC 2013 functions and CEC2017 functions.

Function		GWO	DBO	SCA	AEFA	ASO	PSO	SDGSA
F1	mean	1.59E+003	3.71E–013	1.30E+004	1.43E–013	2.35E–013	2.73E–013	0.00E+000
	std	1.02E+003	2.35E–013	2.20E+003	0.00E+000	7.27E–014	9.25E–014	0.00E+000
F2	mean	2.32E+007	5.11E+006	1.37E+008	3.70E+006	3.53E+005	5.80E+006	2.45E+005
	std	1.49E+007	7.96E+006	4.14E+007	2.57E+006	1.63E+005	4.70E+006	1.34E+005
F3	mean	6.26E+009	1.65E+009	9.40E+010	9.73E+008	1.48E+007	1.78E+008	5.05E+006
	std	4.85E+009	3.92E+009	1.12E+011	3.29E+009	1.69E+007	5.18E+008	5.45E+005
F4	mean	3.17E+004	8.58E+003	3.35E+004	9.91E+004	2.11E+003	5.15E+002	3.97E+001
	std	7.63E+003	3.87E+003	3.95E+003	2.75E+004	1.08E+003	2.84E+002	1.02E+002
F5	mean	9.27E+002	3.41E–012	1.93E+003	2.37E+001	4.35E–012	4.22E–012	3.47E–012
	std	4.34E+002	1.08E–013	3.79E+002	5.74E+001	1.07E–013	7.36E–014	2.27E–012
F6	mean	1.48E+002	2.99E+001	1.36E+003	3.37E+001	3.00E+001	7.48E+001	7.23E+001
	std	3.60E+001	1.52E+001	2.96E+002	2.47E+001	2.43E+001	3.94E+001	1.55E+001
F7	mean	5.90E+001	1.27E+002	3.01E+002	5.67E+001	4.83E+001	5.48E+001	2.04E+001
	std	1.66E+001	3.77E+001	2.96E+002	2.38E+001	1.02E+001	2.28E+001	6.76E+000
F8	mean	2.10E+001	2.09E+001	2.09E+001	2.09E+001	2.09E+001	2.09E+001	2.10E+001
	std	4.97E–002	5.47E–002	5.26E–002	5.73E–002	5.44E–002	8.52E–002	2.09E–002
F9	mean	2.01E+001	3.21E+001	3.85E+001	1.03E+001	4.07E+001	2.26E+001	4.72E+001
	std	3.57E+000	2.95E+000	2.03E+000	2.67E+000	1.29E+000	3.88E+000	3.14E+001
F10	mean	2.98E+002	3.27E+000	1.82E+003	3.27E+001	4.23E–002	1.51E–001	5.43E–003
	std	1.54E+002	1.41E+001	3.01E+002	7.12E+001	3.15E–002	1.13E–001	2.44E–003
F11	mean	9.95E+001	8.86E+001	3.80E+002	2.30E+002	3.98E+001	4.08E+001	1.42E+002
	std	2.63E+001	2.88E+001	2.76E+001	5.13E+001	3.97E+001	1.10E+001	1.82E+002
F12	mean	1.50E+002	2.09E+002	4.00E+002	2.21E+002	6.24E+001	7.57E+001	1.30E+002
	std	6.87E+001	5.70E+001	3.51E+001	1.63E+001	6.55E+001	2.05E+001	1.67E+001
F13	mean	1.97E+002	2.57E+002	3.96E+002	2.19E+002	2.33E+002	2.47E+002	1.87E+002
	std	5.79E+001	4.49E+001	3.55E+001	3.52E+001	5.63E+001	3.23E+001	3.47E+001
F14	mean	2.93E+003	3.58E+003	7.00E+003	3.72E+003	7.61E+003	1.42E+003	3.18E+003
	std	5.29E+002	8.20E+002	3.45E+002	4.35E+002	8.32E+002	2.57E+002	3.60E+002
F15	mean	3.86E+003	5.47E+003	7.19E+003	3.57E+003	6.96E+003	3.74E+003	2.12E+003
	std	1.72E+003	1.14E+003	2.54E+002	7.09E+002	1.41E+003	7.37E+002	3.69E+002
F16	mean	2.55E+000	2.42E+000	2.44E+000	3.86E–002	2.47E+000	1.89E+000	2.16E–003
	std	2.77E–001	3.70E–001	2.32E–001	1.44E–002	2.78E–001	5.05E–001	1.19E–003
F17	mean	1.83E+002	1.80E+002	4.52E+002	9.88E+001	1.27E+002	6.98E+001	4.52E+001

	std	5.31E+001	5.88E+001	4.78E+001	1.67E+001	7.47E+001	1.06E+001	5.20E+000
F18	mean	2.70E+002	2.27E+002	4.34E+002	9.16E+001	1.91E+002	1.18E+002	5.89E+001
	std	5.15E+001	6.22E+001	2.80E+001	1.56E+001	4.68E+001	3.91E+001	5.44E+001
F19	mean	1.37E+003	1.95E+001	5.32E+003	3.82E+000	5.76E+000	3.06E+000	2.15E+000
	std	6.36E+003	9.73E+000	2.49E+003	1.08E+000	5.45E+000	6.68E–001	2.47E+000
F20	mean	1.22E+001	1.29E+001	1.45E+001	1.47E+001	1.46E+001	1.21E+001	1.50E+001
	std	1.42E+000	5.82E–001	3.52E–001	7.52E–001	1.11E+000	2.02E+000	1.50E–010
F21	mean	1.23E+003	3.25E+002	1.80E+003	3.25E+002	3.17E+002	3.11E+002	3.00E+002
	std	3.07E+002	8.01E+001	1.36E+002	9.43E+001	8.00E+001	1.13E+002	3.00E–003
F22	mean	3.23E+003	3.92E+003	7.44E+003	4.35E+003	6.24E+003	1.74E+003	3.38E+003
	std	6.21E+002	1.09E+003	4.55E+002	6.96E+002	2.53E+003	5.02E+002	6.12E+002
F23	mean	4.01E+003	5.45E+003	7.93E+003	3.98E+003	7.18E+003	4.58E+003	5.95E+003
	std	9.84E+002	1.10E+003	3.01E+002	8.06E+002	1.68E+003	8.55E+002	4.56E+003
F24	mean	2.54E+002	2.88E+002	3.20E+002	2.62E+002	2.59E+002	2.58E+002	2.47E+002
	std	9.80E+000	7.83E+000	9.34E+000	1.68E+001	6.67E+000	1.83E+001	2.74E+002
F25	mean	2.72E+002	2.93E+002	3.67E+002	3.57E+002	3.13E+002	3.01E+002	2.63E+002
	std	7.17E+000	8.72E+000	9.11E+000	7.30E+000	3.60E+001	2.26E+001	3.06E+002
F26	mean	3.19E+002	2.54E+002	2.11E+002	3.15E+002	2.00E+002	3.17E+002	2.15E+002
	std	5.99E+001	8.28E+001	3.72E+000	4.65E+001	8.07E–003	6.59E+001	3.34E+001
F27	mean	8.21E+002	1.11E+003	1.32E+003	6.50E+002	5.98E+002	8.72E+002	1.17E+003
	std	7.62E+001	8.90E+001	7.99E+001	6.72E+001	8.74E+001	1.27E+002	9.04E+002
F28	mean	1.45E+003	8.11E+002	2.94E+003	3.95E+002	3.00E+002	5.45E+002	2.66E+003
	std	5.16E+002	8.33E+002	2.74E+002	3.39E+002	2.62E+002	5.21E+002	2.80E+003
F29	mean	1.55E+009	3.57E+004	1.27E+010	1.55E+003	4.08E+005	2.95E+003	4.99E+002
	std	1.21E+009	6.43E+004	2.43E+009	1.39E+003	9.80E+005	2.74E+003	2.98E+002
F31	mean	3.24E+004	5.55E+003	3.48E+004	1.80E+005	3.37E+002	3.00E+002	3.00E+002
	std	1.07E+004	4.73E+003	5.86E+003	1.82E+004	8.11E+001	8.92E–007	6.71E–011
F32	mean	4.70E+002	5.28E+002	2.13E+003	5.71E+002	4.80E+002	5.03E+002	4.27E+002
	std	5.34E+001	4.26E+001	4.30E+002	4.55E+001	3.18E+001	5.40E+001	2.14E+001
F33	mean	9.92E+001	7.03E+002	7.86E+002	5.66E+002	5.98E+002	6.00E+002	6.63E+002
	std	2.13E+001	6.37E+001	2.26E+001	1.21E+001	3.53E+001	3.05E+001	3.67E+001
F34	mean	6.74E+000	6.29E+002	6.54E+002	6.00E+002	6.08E+002	6.01E+002	6.52E+002
	std	3.72E+000	1.49E+001	5.66E+000	1.56E–001	9.08E+000	1.33E+000	3.07E+000
F35	mean	9.57E+002	9.15E+002	1.10E+003	9.82E+002	8.31E+002	8.02E+002	7.85E+002
	std	4.53E+001	9.42E+001	2.50E+001	7.46E+000	2.48E+001	1.82E+001	1.60E+001
F36	mean	8.90E+001	9.90E+002	1.06E+003	8.61E+002	8.91E+002	8.81E+002	9.28E+002
	std	1.90E+001	5.95E+001	1.99E+001	1.09E+001	2.42E+001	2.22E+001	2.77E+001
F37	mean	1.08E+003	3.42E+003	5.16E+003	9.01E+002	1.63E+003	1.06E+003	3.73E+003
	std	7.66E+002	2.17E+003	9.55E+002	5.36E+000	8.21E+002	4.55E+002	1.50E+003
F38	mean	3.07E+003	5.42E+003	8.05E+003	5.04E+003	4.57E+003	4.14E+003	4.09E+003
	std	1.02E+003	1.03E+003	2.72E+002	5.93E+002	7.91E+002	5.41E+002	4.66E+002
F39	mean	7.28E+002	1.42E+003	2.03E+003	2.17E+003	1.24E+003	1.22E+003	1.20E+003
	std	8.22E+002	8.75E+001	1.96E+002	4.39E+002	4.04E+001	4.35E+001	6.51E+001
F40	mean	6.12E+007	1.48E+007	1.59E+009	3.41E+006	1.01E+006	1.45E+005	1.46E+004

	std	8.02E+007	1.84E+007	4.13E+008	1.93E+006	9.70E+005	3.63E+005	3.52E+004
F41	mean	5.44E+006	7.21E+005	5.27E+008	4.11E+004	8.71E+004	1.59E+004	1.60E+004
	std	2.08E+007	1.06E+006	2.02E+008	1.72E+004	4.44E+004	1.51E+004	8.50E+003
F42	mean	2.63E+005	4.67E+004	1.70E+005	5.22E+005	1.11E+004	9.16E+003	2.02E+003
	std	5.20E+005	4.87E+004	1.43E+005	3.18E+005	1.06E+004	2.54E+004	1.27E+003
F43	mean	1.98E+005	1.66E+005	4.56E+006	1.63E+004	4.94E+004	8.58E+003	3.91E+003
	std	5.12E+005	2.08E+005	2.83E+006	5.48E+003	2.85E+004	6.35E+003	1.52E+004
F44	mean	3.82E+003	3.71E+003	3.79E+003	3.65E+003	4.36E+003	3.43E+003	3.12E+003
	std	2.60E+002	3.39E+002	3.05E+002	2.51E+002	2.64E+002	2.93E+002	3.05E+002
F45	mean	2.56E+002	2.30E+003	2.36E+003	3.04E+003	1.99E+003	1.93E+003	2.43E+003
	std	1.26E+002	2.07E+002	1.84E+002	2.75E+002	1.46E+002	1.29E+002	1.79E+002
F46	mean	6.51E+005	1.11E+006	2.04E+006	1.47E+006	1.65E+005	5.90E+004	4.67E+004
	std	7.64E+005	1.14E+006	1.47E+006	5.48E+005	1.31E+005	3.44E+004	1.42E+004
F47	mean	5.09E+005	1.48E+005	1.75E+007	2.93E+004	7.11E+004	8.11E+003	6.75E+003
	std	6.62E+005	2.67E+005	9.36E+006	1.33E+004	1.30E+005	7.06E+003	3.80E+003
F48	mean	3.93E+002	2.49E+003	2.56E+003	2.79E+003	2.34E+003	2.30E+003	2.63E+003
	std	1.20E+002	1.71E+002	1.24E+002	2.64E+002	1.06E+002	1.14E+002	1.29E+002
F49	mean	2.91E+002	2.53E+003	2.57E+003	2.37E+003	2.39E+003	2.38E+003	2.53E+003
	std	3.35E+001	5.51E+001	1.90E+001	1.66E+001	3.28E+001	2.59E+001	4.25E+001
F50	mean	2.83E+003	3.25E+003	3.83E+003	3.30E+003	3.01E+003	4.35E+003	2.30E+003
	std	1.84E+003	1.12E+003	1.60E+002	9.63E–013	1.67E+003	1.89E+003	2.45E+001
F51	mean	4.53E+002	2.91E+003	3.14E+003	2.81E+003	2.74E+003	2.77E+003	3.19E+003
	std	3.98E+001	8.22E+001	6.29E+001	2.70E+001	3.28E+001	4.42E+001	1.09E+002
F52	mean	5.23E+002	3.06E+003	3.33E+003	2.94E+003	2.90E+003	2.90E+003	3.05E+003
	std	5.23E+001	8.62E+001	5.45E+001	1.66E+001	2.68E+001	4.77E+001	1.10E+002
F53	mean	4.90E+002	2.91E+003	3.24E+003	3.05E+003	2.92E+003	2.91E+003	2.89E+003
	std	3.74E+001	2.55E+001	5.04E+001	2.76E+001	1.52E+001	1.59E+001	2.34E+001
F54	mean	1.99E+003	5.64E+003	7.05E+003	2.90E+003	3.88E+003	3.96E+003	6.56E+003
	std	4.18E+002	8.40E+002	1.08E+003	1.06E–012	9.52E+002	1.15E+003	2.52E+003
F55	mean	5.43E+002	3.29E+003	3.74E+003	3.36E+003	3.24E+003	3.31E+003	3.23E+003
	std	2.60E+001	5.03E+001	8.85E+001	4.85E+001	1.50E+001	3.92E+001	2.50E+001
F56	mean	6.10E+002	3.31E+003	3.97E+003	3.29E+003	3.17E+003	3.59E+003	3.16E+003
	std	7.10E+001	1.72E+002	1.32E+002	2.69E+001	4.99E+001	8.18E+001	1.91E+001
F57	mean	3.88E+003	4.18E+003	4.82E+003	4.67E+003	3.70E+003	3.65E+003	2.14E+003
	std	2.13E+002	2.87E+002	2.16E+002	3.77E+002	1.60E+002	1.73E+002	1.48E+002
F58	mean	6.24E+006	2.74E+006	6.62E+007	2.60E+007	1.52E+005	1.92E+004	1.16E+004
	std	6.37E+006	4.98E+006	2.80E+007	5.72E+006	2.82E+005	9.67E+003	1.01E+004

Table A2

Results of SDGSA with MRFO, ISA, FDA, ABC and SMA for the 30-dimensional CEC 2013 functions and CEC2017 functions.

Function		MRFO	ISA	FDA	ABC	SMA	SDGSA
F1	mean	5.46E–013	7.03E–012	2.96E–013	4.32E–013	8.29E–004	0.00E+000
	std	2.36E–013	1.07E–011	1.22E–013	6.94E–014	2.97E–004	0.00E+000
F2	mean	5.79E+005	5.27E+005	5.09E+005	6.90E+006	3.22E+006	2.45E+005
	std	2.57E+005	3.29E+005	3.23E+005	2.65E+006	1.28E+006	1.34E+005
F3	mean	9.91E+007	1.07E+009	5.22E+008	4.67E+008	7.28E+008	5.05E+006
	std	1.41E+008	1.27E+009	5.99E+008	3.74E+008	1.08E+009	5.45E+005
F4	mean	1.51E+003	1.12E+002	7.03E+001	9.55E+004	6.77E+001	3.97E+001
	std	1.62E+003	1.95E+002	6.71E+001	9.12E+003	7.11E+001	1.02E+002
F5	mean	6.67E–012	8.17E–001	3.68E–012	6.78E–012	7.85E–003	3.47E–012
	std	7.60E–013	3.13E+000	1.18E–013	8.70E–014	1.63E–003	2.27E–012
F6	mean	2.44E+001	2.27E+001	1.87E+001	1.54E+001	8.01E+001	7.23E+001
	std	2.38E+001	2.73E+001	2.16E+001	3.12E+000	2.11E+001	1.55E+001
F7	mean	1.03E+002	7.29E+001	1.25E+002	1.24E+002	9.39E+001	2.04E+001
	std	2.51E+001	1.61E+001	3.32E+001	2.08E+001	3.58E+001	6.76E+000
F8	mean	2.10E+001	2.10E+001	2.10E+001	2.09E+001	2.10E+001	2.10E+001
	std	6.06E–002	5.82E–002	5.58E–002	5.50E–002	3.90E–002	2.09E–002
F9	mean	2.99E+001	3.35E+001	3.28E+001	3.04E+001	4.32E+001	4.72E+001
	std	3.74E+000	3.43E+000	2.87E+000	1.37E+000	3.36E+000	3.14E+001
F10	mean	1.69E–001	2.63E–001	4.88E–002	4.61E–001	4.71E–001	5.43E–003
	std	8.97E–002	1.80E–001	3.15E–002	1.78E–001	2.50E–001	2.44E–003
F11	mean	1.91E+002	9.52E+001	1.09E+002	5.87E–014	9.06E+000	1.42E+002
	std	6.04E+001	2.39E+001	2.46E+001	1.04E–014	2.75E+000	1.82E+002
F12	mean	2.21E+002	9.60E+001	2.60E+002	3.13E+002	1.38E+002	1.30E+002
	std	8.73E+001	2.24E+001	6.24E+001	6.09E+001	2.76E+001	1.67E+001
F13	mean	3.14E+002	2.65E+002	2.73E+002	3.42E+002	1.89E+002	1.87E+002
	std	5.73E+001	2.12E+001	3.54E+001	4.21E+001	4.28E+001	3.47E+001
F14	mean	2.69E+003	3.84E+003	2.61E+003	2.73E–001	1.24E+003	3.18E+003
	std	6.83E+002	6.59E+002	7.33E+002	2.74E–001	3.08E+002	3.60E+002
F15	mean	4.14E+003	4.36E+003	4.40E+003	3.84E+003	3.90E+003	2.12E+003
	std	7.08E+002	7.96E+002	7.25E+002	3.67E+002	7.56E+002	3.69E+002
F16	mean	2.25E+000	1.74E+000	1.51E+000	1.02E+000	7.35E–001	2.16E–003
	std	4.07E–001	3.93E–001	5.65E–001	1.92E–001	2.75E–001	1.19E–003
F17	mean	2.39E+002	7.54E+001	1.71E+002	5.95E+001	5.02E+001	4.52E+001
	std	8.37E+001	1.59E+001	4.56E+001	4.92E+000	5.84E+000	5.20E+000
F18	mean	2.25E+002	8.12E+001	2.41E+002	2.99E+002	1.42E+002	5.89E+001
	std	6.03E+001	1.86E+001	5.38E+001	3.19E+001	2.07E+001	5.44E+001
F19	mean	1.35E+001	8.70E+000	1.36E+001	2.66E+000	2.74E+000	2.15E+000
	std	5.09E+000	2.62E+000	4.37E+000	7.35E–002	7.31E–001	2.47E+000
F20	mean	1.28E+001	1.17E+001	1.35E+001	1.46E+001	1.50E+001	1.50E+001
	std	8.38E–001	9.01E–001	8.06E–001	2.28E–001	3.40E–006	1.50E–010
F21	mean	3.17E+002	3.96E+002	3.17E+002	3.67E+002	3.26E+002	3.00E+002
	std	6.27E+001	5.28E+001	6.80E+001	4.24E+001	8.60E+001	3.00E–003
F22	mean	3.33E+003	4.79E+003	2.77E+003	2.83E+001	1.33E+003	3.38E+003

	std	1.15E+003	8.41E+002	8.17E+002	2.97E+001	3.44E+002	6.12E+002
F23	mean	5.02E+003	4.72E+003	5.55E+003	5.12E+003	6.29E+003	5.95E+003
	std	8.25E+002	7.43E+002	7.89E+002	4.76E+002	8.20E+002	4.56E+003
F24	mean	2.87E+002	2.62E+002	2.90E+002	2.93E+002	2.64E+002	2.47E+002
	std	1.18E+001	1.01E+001	1.08E+001	6.54E+000	6.34E+000	2.74E+002
F25	mean	3.10E+002	3.13E+002	2.97E+002	3.08E+002	2.75E+002	2.63E+002
	std	1.32E+001	1.84E+001	8.58E+000	5.00E+000	8.88E+000	3.06E+002
F26	mean	2.00E+002	2.00E+002	2.18E+002	2.01E+002	2.00E+002	2.15E+002
	std	4.52E–002	1.86E–002	5.62E+001	2.15E–001	1.98E–001	3.34E+001
F27	mean	1.11E+003	1.01E+003	1.14E+003	4.78E+002	1.21E+003	1.17E+003
	std	8.94E+001	1.79E+002	8.97E+001	2.35E+002	8.13E+001	9.04E+002
F28	mean	2.05E+003	3.00E+002	5.22E+002	2.12E+002	3.00E+002	2.66E+003
	std	1.34E+003	5.62E+003	7.09E+002	9.59E+001	3.15E+001	2.80E+003
F29	mean	3.11E+003	8.72E+002	1.05E+003	8.89E+002	5.90E+003	4.99E+002
	std	4.12E+003	1.02E+003	9.65E+002	1.65E+002	5.55E+003	2.98E+002
F31	mean	3.00E+002	3.00E+002	3.00E+002	1.17E+005	3.00E+002	3.00E+002
	std	3.89E–004	4.28E–002	1.99E–004	2.40E+004	6.09E–003	6.71E–011
F32	mean	4.52E+002	4.35E+002	4.24E+002	4.30E+002	4.88E+002	4.27E+002
	std	2.93E+001	3.67E+001	2.97E+001	2.85E+001	8.40E+000	2.14E+001
F33	mean	6.88E+002	5.95E+002	6.80E+002	5.95E+002	6.61E+002	6.63E+002
	std	4.26E+001	2.95E+001	4.87E+001	1.73E+001	1.94E+001	3.67E+001
F34	mean	6.27E+002	6.11E+002	6.18E+002	6.00E+002	6.01E+002	6.52E+002
	std	1.34E+001	4.28E+000	8.79E+000	5.17E–014	7.16E–001	3.07E+000
F35	mean	1.05E+003	8.81E+002	9.68E+002	8.04E+002	8.30E+002	7.85E+002
	std	1.06E+002	1.54E+001	5.51E+001	1.06E+001	1.71E+001	1.60E+001
F36	mean	9.41E+002	8.95E+002	9.40E+002	8.98E+002	9.88E+002	9.28E+002
	std	3.02E+001	2.41E+001	3.17E+001	1.84E+001	2.47E+001	2.77E+001
F37	mean	3.92E+003	1.06E+003	3.52E+003	1.92E+003	3.83E+003	3.73E+003
	std	9.44E+002	8.51E+001	1.07E+003	5.60E+002	1.79E+003	1.50E+003
F38	mean	4.95E+003	5.04E+003	5.31E+003	4.35E+003	4.16E+003	4.09E+003
	std	6.93E+002	6.08E+002	7.08E+002	3.56E+002	5.88E+002	4.66E+002
F39	mean	1.39E+003	1.29E+003	1.23E+003	1.47E+003	1.23E+003	1.20E+003
	std	3.45E+001	3.25E+001	4.74E+001	4.61E+002	5.48E+001	6.51E+001
F40	mean	3.51E+004	1.84E+004	2.99E+004	5.57E+005	8.44E+005	1.46E+004
	std	2.29E+004	1.03E+004	2.50E+004	4.59E+005	6.36E+005	3.52E+003
F41	mean	2.29E+004	2.05E+004	1.90E+004	2.56E+004	3.71E+004	1.60E+004
	std	1.76E+004	5.65E+003	1.06E+004	2.97E+003	2.69E+004	8.50E+003
F42	mean	3.61E+003	2.85E+003	3.64E+003	1.01E+005	3.21E+004	2.02E+003
	std	2.14E+003	4.24E+002	8.01E+001	9.63E+004	1.65E+004	1.27E+003
F43	mean	6.80E+003	7.87E+003	3.99E+003	2.25E+003	2.82E+004	3.91E+003
	std	7.70E+003	6.80E+003	3.80E+003	7.33E+002	1.41E+004	1.52E+004
F44	mean	5.64E+003	3.46E+003	4.62E+003	3.60E+003	3.40E+003	3.12E+003
	std	2.81E+002	2.76E+002	2.64E+002	1.54E+002	3.48E+002	3.05E+002
F45	mean	2.26E+003	1.95E+003	2.18E+003	1.96E+003	2.57E+003	2.43E+003

	std	2.02E+002	1.33E+002	1.72E+002	9.85E+001	1.66E+002	1.79E+002
F46	mean	8.64E+004	5.93E+004	5.55E+004	1.66E+005	1.98E+005	4.67E+004
	std	4.25E+004	3.05E+004	2.15E+004	8.61E+004	8.58E+004	1.42E+004
F47	mean	1.04E+004	7.98E+003	8.40E+003	7.93E+003	3.98E+004	6.75E+003
	std	1.13E+004	6.87E+003	4.17E+003	9.49E+002	1.99E+004	3.80E+003
F48	mean	2.50E+003	2.49E+003	2.52E+003	2.26E+003	2.38E+003	2.63E+003
	std	2.16E+002	1.84E+002	2.10E+002	1.02E+002	1.74E+002	1.29E+002
F49	mean	2.43E+003	2.39E+003	2.44E+003	2.38E+003	2.39E+003	2.53E+003
	std	5.30E+001	2.63E+001	4.24E+001	6.21E+001	2.56E+001	4.25E+001
F50	mean	2.60E+003	2.31E+003	4.85E+003	3.19E+003	5.01E+003	2.30E+003
	std	1.15E+003	8.85E+000	2.33E+003	1.38E+003	1.44E+003	2.45E+001
F51	mean	2.83E+003	2.78E+003	2.81E+003	2.73E+003	2.74E+003	3.19E+003
	std	6.19E+001	3.02E+001	4.72E+001	3.05E+001	2.10E+001	1.09E+002
F52	mean	3.00E+003	2.94E+003	2.99E+003	2.92E+003	2.93E+003	3.05E+003
	std	6.70E+001	2.97E+001	4.22E+001	2.21E+002	2.51E+001	1.10E+002
F53	mean	2.90E+003	2.90E+003	2.90E+003	2.91E+003	2.99E+003	2.89E+003
	std	2.14E+001	2.01E+001	1.58E+001	1.21E+000	2.37E+000	2.34E+001
F54	mean	5.38E+003	4.69E+003	4.54E+003	2.94E+003	4.57E+003	6.56E+003
	std	1.86E+003	9.35E+002	1.23E+003	2.73E+002	3.11E+002	2.52E+003
F55	mean	3.29E+003	3.26E+003	3.24E+003	3.31E+003	3.32E+003	3.23E+003
	std	3.19E+001	2.42E+001	1.69E+001	5.71E+000	1.21E+001	2.50E+001
F56	mean	3.19E+003	3.24E+003	3.32E+003	3.20E+003	3.21E+003	3.16E+003
	std	4.80E+001	5.73E+001	4.93E+001	3.62E+000	5.44E+001	1.91E+001
F57	mean	3.92E+003	3.85E+003	3.80E+003	3.57E+003	3.75E+003	2.14E+003
	std	2.22E+002	1.96E+002	2.27E+002	1.03E+002	1.92E+002	1.48E+002
F58	mean	1.21E+005	1.77E+004	2.74E+004	1.83E+004	1.73E+004	1.16E+004
	std	3.21E+003	2.20E+003	1.84E+003	1.62E+003	4.98E+003	1.01E+004

Table A3

Results of SDGSA with GWO, DBO, SCA, AEFA, ASO and PSO for the 50-dimensional CEC 2013 functions.

Function		GWO	DBO	SCA	AEFA	ASO	PSO	SDGSA
F1	mean	5.05E+003	9.55E–013	3.04E+004	2.12E–013	6.21E–13	2.95E–012	0.00E+000
	std	2.01E+003	1.02E–012	3.02E+003	5.77E–014	2.92E–013	5.87E–012	0.00E+000
F2	mean	4.63E+007	1.12E+007	4.17E+008	9.52E+006	2.99E+006	1.55E+007	2.04E+006
	std	1.97E+007	1.30E+007	1.13E+008	5.86E+006	3.74E+005	1.54E+007	1.20E+006
F3	mean	2.32E+010	1.31E+010	8.42E+010	2.38E+009	3.10E+008	4.90E+008	1.48E+007
	std	7.22E+009	2.08E+010	1.40E+010	4.60E+009	5.82E+008	5.80E+008	1.76E+006
F4	mean	4.70E+004	2.89E+004	5.89E+004	1.47E+005	1.74E+004	2.45E+003	9.01E+003
	std	6.69E+003	9.49E+003	6.34E+003	4.14E+004	2.34E+003	1.04E+003	3.96E+003
F5	mean	1.26E+003	2.77E–010	2.89E+003	6.56E+001	5.76E–011	7.22E–011	1.36E–011

	std	7.19E+002	3.95E–012	5.20E+002	1.17E+002	1.66E–013	2.02E–011	1.04E–011
F6	mean	3.51E+002	7.99E+001	2.06E+003	1.06E+002	6.43E+001	7.64E+001	4.97E+001
	std	1.08E+002	2.68E+001	3.17E+002	1.44E+002	1.91E+001	2.92E+001	2.95E+001
F7	mean	1.69E+002	1.37E+002	1.94E+002	1.76E+002	1.46E+002	1.64E+002	1.20E+002
	std	1.24E+001	2.66E+001	2.89E+001	2.14E+001	1.07E+001	1.94E+001	3.69E+001
F8	mean	2.12E+001	2.11E+001	2.11E+001	2.11E+001	2.11E+001	2.11E+001	2.10E+001
	std	3.08E–002	3.89E–002	4.37E–002	3.70E–002	4.82E–002	4.52E–002	6.65E–002
F9	mean	3.91E+001	6.25E+001	7.00E+001	3.96E+001	6.68E+001	4.03E+001	2.59E+001
	std	4.71E+000	3.12E+000	2.82E+000	2.63E+000	1.43E+001	4.66E+000	3.26E+000
F10	mean	8.54E+002	6.47E+000	3.86E+003	1.50E+002	5.04E+000	7.88E–001	2.89E–001
	std	2.96E+002	1.47E+001	4.59E+002	1.68E+002	3.47E–002	3.97E–002	2.94E–001
F11	mean	2.68E+002	1.78E+002	7.12E+002	3.07E+002	1.13E+002	1.26E+002	2.61E+002
	std	3.74E+001	5.03E+001	3.77E+001	4.54E+001	7.05E+001	3.25E+001	9.85E+001
F12	mean	2.94E+002	4.22E+002	7.72E+002	4.65E+002	3.18E+002	3.66E+002	2.46E+002
	std	6.75E+001	1.13E+002	4.58E+001	2.76E+001	6.51E+001	3.56E+001	6.68E+000
F13	mean	5.08E+002	5.52E+002	7.75E+002	3.95E+002	4.80E+002	4.16E+002	3.78E+002
	std	9.19E+001	9.75E+001	5.85E+001	6.71E+001	8.85E+001	6.21E+001	9.18E+001
F14	mean	5.71E+003	6.94E+003	1.34E+004	6.95E+003	1.37E+004	3.01E+003	3.99E+003
	std	1.59E+003	1.85E+003	4.97E+002	1.11E+003	2.44E+003	6.48E+002	5.79E+002
F15	mean	7.99E+003	1.14E+004	1.44E+004	6.98E+003	1.47E+004	7.39E+003	4.05E+003
	std	3.00E+003	2.41E+003	3.70E+002	8.66E+002	3.54E+002	1.02E+003	8.59E+002
F16	mean	3.49E+000	3.49E+000	3.48E+000	2.52E+000	3.48E+000	2.81E+000	2.03E+000
	std	3.31E–001	3.00E–001	3.32E–001	2.74E–002	2.41E–001	4.54E–001	2.45E–001
F17	mean	3.79E+002	3.79E+002	8.94E+002	2.01E+002	2.91E+002	1.65E+002	3.03E+002
	std	7.18E+001	8.06E+001	6.39E+001	4.19E+001	1.67E+002	2.44E+001	3.55E+001
F18	mean	5.81E+002	4.27E+002	8.99E+002	2.15E+002	3.52E+002	2.37E+002	3.99E+002
	std	8.01E+001	1.26E+002	5.30E+001	7.18E+001	1.45E+002	7.94E+001	1.67E+002
F19	mean	3.33E+003	5.21E+001	3.38E+004	1.77E+001	1.07E+001	1.87E+001	1.22E+001
	std	5.75E+003	2.38E+001	1.75E+004	1.83E+000	9.11E+000	2.96E+000	1.47E+000
F20	mean	2.10E+001	2.31E+001	2.40E+001	2.40E+001	2.34E+001	2.12E+001	1.50E+001
	std	9.11E–001	1.04E+000	6.10E–001	1.08E+000	2.14E+000	1.91E+000	4.41E–011
F21	mean	2.68E+003	8.83E+002	3.76E+003	7.55E+002	9.14E+002	9.16E+002	3.72E+002
	std	6.27E+002	3.36E+002	1.06E+002	3.32E+002	3.12E+002	2.79E+002	8.29E+001
F22	mean	6.75E+003	6.76E+003	1.48E+004	7.55E+003	1.34E+004	4.95E+003	4.46E+003
	std	8.40E+002	1.60E+003	6.64E+002	1.07E+003	3.77E+003	1.32E+003	7.49E+002
F23	mean	8.37E+003	1.11E+004	1.54E+004	7.42E+003	1.47E+004	1.01E+004	4.71E+003
	std	1.27E+003	2.09E+003	3.91E+002	1.41E+003	2.31E+003	1.81E+003	7.30E+002
F24	mean	3.07E+002	3.69E+002	4.72E+002	2.99E+002	2.97E+002	3.20E+002	2.88E+002
	std	8.97E+000	1.00E+001	1.41E+001	1.26E+001	1.08E+001	2.41E+001	9.73E+000
F25	mean	3.55E+002	3.82E+002	5.45E+002	3.68E+002	4.52E+002	4.14E+002	3.08E+002
	std	1.15E+001	1.20E+001	1.12E+001	1.28E+001	2.65E+001	1.73E+001	8.32E+000
F26	mean	3.95E+002	3.55E+002	2.48E+002	3.64E+002	2.95E+002	3.78E+002	2.15E+002
	std	3.69E+001	1.28E+002	1.55E+001	3.24E+001	9.70E+001	8.15E+001	2.78E+000
F27	mean	1.36E+003	1.93E+003	2.43E+003	1.11E+003	1.20E+003	1.57E+003	9.54E+002

	std	1.25E+002	1.10E+002	7.85E+001	1.17E+002	1.37E+002	1.37E+002	6.69E+001
F28	mean	2.27E+003	1.70E+003	5.81E+003	1.63E+003	6.24E+002	8.22E+002	3.24E+003
	std	1.04E+003	1.87E+003	5.31E+002	1.52E+003	8.53E+002	1.09E+003	6.55E+002
F29	mean	9.31E+009	6.21E+006	4.42E+010	2.82E+003	4.32E+005	8.04E+003	1.80E+003
	std	3.45E+009	8.35E+006	4.90E+009	1.89E+003	5.91E+005	7.89E+003	1.52E+003
F31	mean	8.17E+004	1.10E+005	1.03E+005	1.83E+005	2.48E+004	1.71E+003	3.13E+002
	std	1.45E+004	1.77E+004	1.17E+004	1.74E+004	8.85E+003	1.18E+003	2.18E+000
F32	mean	1.04E+003	6.79E+002	9.22E+003	6.65E+002	6.87E+002	6.33E+002	5.94E+002
	std	6.45E+002	7.90E+001	1.36E+003	4.07E+001	4.37E+001	7.45E+001	3.38E+001
F33	mean	2.10E+002	9.15E+002	1.06E+003	5.62E+002	7.17E+002	7.00E+002	8.43E+002
	std	3.77E+001	1.15E+002	3.11E+001	1.17E+001	4.04E+001	4.61E+001	5.96E+001
F34	mean	1.69E+001	6.56E+002	6.74E+002	6.00E+002	6.29E+002	6.11E+002	6.60E+002
	std	4.36E+000	1.49E+001	5.64E+000	1.25E+001	1.00E+001	1.03E+001	1.81E+000
F35	mean	3.70E+002	1.20E+003	1.57E+003	8.80E+002	9.95E+002	9.05E+002	7.46E+002
	std	6.84E+001	1.54E+002	6.44E+001	6.31E+000	6.91E+001	2.67E+001	2.38E+000
F36	mean	1.22E+003	1.19E+003	1.37E+003	1.87E+003	1.02E+003	9.97E+002	8.47E+002
	std	3.65E+001	1.17E+002	2.91E+001	1.62E+001	5.13E+001	5.07E+001	1.64E+001
F37	mean	6.24E+003	1.44E+004	2.46E+004	1.91E+003	7.98E+003	4.18E+003	9.00E+002
	std	3.05E+003	6.47E+003	2.98E+003	2.67E+001	4.75E+003	3.35E+003	8.72E–001
F38	mean	5.89E+003	9.99E+003	1.41E+004	5.01E+003	7.24E+003	6.55E+003	3.81E+003
	std	1.27E+003	1.38E+003	4.79E+002	5.91E+002	9.79E+002	9.19E+002	2.84E+002
F39	mean	3.87E+003	1.69E+003	6.77E+003	1.94E+003	1.30E+003	1.32E+003	1.00E+003
	std	2.39E+003	1.27E+002	7.49E+002	2.66E+002	5.32E+001	5.51E+001	8.78E+000
F40	mean	1.37E+009	1.08E+008	1.44E+010	3.48E+006	4.49E+006	1.75E+006	3.88E+005
	std	1.93E+009	8.44E+007	3.12E+009	1.39E+006	3.51E+006	3.55E+006	1.79E+005
F41	mean	1.54E+008	1.51E+006	2.97E+009	3.93E+004	1.31E+005	2.12E+004	2.52E+003
	std	1.53E+008	1.43E+006	1.22E+009	1.51E+004	7.13E+004	7.80E+004	7.56E+002
F42	mean	8.80E+005	6.99E+005	2.85E+006	4.91E+005	6.23E+004	4.19E+004	2.36E+004
	std	1.07E+006	5.47E+005	1.16E+006	3.20E+005	3.59E+004	8.60E+004	2.16E+004
F43	mean	1.41E+007	7.17E+005	3.33E+008	1.76E+004	4.39E+004	1.01E+004	2.32E+003
	std	1.78E+007	3.12E+006	8.63E+007	7.27E+003	2.82E+004	9.91E+003	2.44E+002
F44	mean	1.97E+003	4.02E+003	5.78E+003	2.67E+003	2.99E+003	2.91E+003	1.62E+003
	std	4.13E+002	5.29E+002	2.88E+002	3.72E+002	4.57E+002	4.37E+002	2.68E+002
F45	mean	1.03E+003	3.74E+003	4.16E+003	3.09E+003	2.85E+003	2.74E+003	3.01E+003
	std	2.99E+002	3.34E+002	1.83E+002	3.01E+002	3.17E+002	2.85E+002	2.26E+002
F46	mean	4.25E+006	2.71E+006	1.33E+007	1.47E+006	3.39E+005	1.03E+006	7.41E+004
	std	5.22E+006	2.93E+006	5.73E+006	6.23E+005	3.02E+005	2.04E+006	4.26E+004
F47	mean	2.87E+006	9.40E+005	1.97E+008	2.64E+004	9.81E+004	1.70E+004	1.66E+004
	std	5.53E+006	9.36E+005	7.63E+007	8.11E+003	1.37E+005	8.93E+003	6.45E+003
F48	mean	8.43E+002	3.39E+003	3.70E+003	2.77E+003	2.92E+003	2.71E+003	3.20E+003
	std	2.61E+002	3.43E+002	1.88E+002	3.14E+002	2.94E+002	3.57E+002	1.59E+002
F49	mean	4.12E+002	2.73E+003	2.90E+003	2.37E+003	2.50E+003	2.48E+003	2.75E+003
	std	4.94E+001	1.16E+002	3.53E+001	1.55E+001	2.82E+001	4.60E+001	8.36E+001
F50	mean	7.00E+003	1.08E+004	1.50E+004	2.90E+003	8.53E+003	8.81E+003	2.62E+003

	std	1.92E+003	1.97E+003	2.10E+003	9.29E+002	1.21E+003	1.12E+003	8.62E+002
F51	mean	6.74E+002	3.31E+003	3.88E+003	3.24E+003	2.93E+003	2.99E+003	3.86E+003
	std	5.46E+001	1.71E+002	6.87E+001	2.26E+001	4.14E+001	6.03E+001	2.37E+002
F52	mean	7.64E+002	3.48E+003	4.17E+003	2.94E+003	3.11E+003	3.13E+003	3.00E+003
	std	9.18E+001	1.88E+002	1.23E+002	1.78E+001	7.86E+001	1.21E+002	2.93E+001
F53	mean	1.21E+003	3.10E+003	6.71E+003	3.06E+003	3.06E+003	3.13E+003	3.01E+003
	std	3.41E+002	5.78E+001	7.53E+002	2.35E+001	3.32E+001	3.38E+001	1.11E+001
F54	mean	4.87E+003	7.31E+003	1.31E+004	4.99E+003	4.91E+003	5.40E+003	4.84E+003
	std	6.46E+002	2.00E+003	8.46E+002	3.35E+002	1.56E+003	1.71E+003	3.36E+003
F55	mean	9.06E+002	3.83E+003	5.39E+003	3.35E+003	3.59E+003	3.72E+003	4.83E+003
	std	1.10E+002	2.69E+002	2.63E+002	4.36E+001	2.80E+002	1.37E+002	1.15E+003
F56	mean	1.54E+003	4.34E+003	7.09E+003	3.30E+003	3.30E+003	3.40E+003	3.41E+003
	std	4.07E+002	2.07E+003	4.49E+002	1.86E+001	3.46E+001	6.59E+001	2.43E+001
F57	mean	4.58E+003	5.53E+003	7.65E+003	4.71E+003	4.31E+003	4.69E+003	4.22E+003
	std	3.56E+002	8.97E+002	6.16E+002	3.45E+002	2.87E+002	2.96E+002	1.74E+002
F58	mean	1.03E+008	1.79E+007	5.43E+008	2.63E+007	5.74E+006	9.72E+006	1.69E+006
	std	4.09E+007	1.11E+007	1.37E+008	5.81E+006	2.42E+006	6.73E+006	4.91E+005

Table A4

Results of SDGSA with MRFO, ISA, FDA, ABC and SMA for the 50-dimensional CEC 2013 functions and CEC2017 functions.

Function		MRFO	ISA	FDA	ABC	SMA	SDGSA
F1	mean	4.82E–012	2.84E–008	9.93E–013	9.32E–013	4.55E–003	0.00E+000
	std	1.15E–011	8.81E–008	4.11E–013	1.38E–013	1.38E–003	0.00E+000
F2	mean	2.32E+006	2.78E+006	3.11E+006	1.62E+007	7.82E+006	2.04E+006
	std	4.42E+005	6.16E+005	6.61E+005	3.43E+006	2.36E+006	1.20E+006
F3	mean	4.34E+008	1.74E+009	2.49E+009	3.99E+009	2.06E+009	1.48E+007
	std	3.44E+008	1.90E+009	2.26E+009	2.56E+009	1.98E+009	1.76E+006
F4	mean	1.26E+004	2.36E+004	1.12E+004	1.70E+005	3.54E+004	9.01E+003
	std	4.30E+003	3.43E+002	7.00E+002	2.14E+004	1.86E+002	3.96E+003
F5	mean	4.60E–011	1.32E+000	5.59E–010	1.38E–010	3.18E–002	1.36E–011
	std	1.14E–011	4.84E+000	5.47E–010	1.64E–013	4.55E–003	1.04E–011
F6	mean	6.95E+001	6.43E+001	6.24E+001	8.20E+001	7.59E+001	4.97E+001
	std	3.36E+001	2.51E+001	2.32E+001	4.58E+000	2.06E+001	2.95E+001
F7	mean	1.07E+002	1.81E+002	1.31E+002	1.74E+002	1.47E+002	1.20E+002
	std	1.77E+001	1.02E+001	2.16E+001	1.86E+001	2.86E+001	3.69E+001
F8	mean	2.11E+001	2.11E+001	2.12E+001	2.12E+001	2.11E+001	2.10E+001
	std	3.13E–002	3.64E–002	4.57E–002	3.09E–002	2.99E–002	6.65E–002
F9	mean	5.50E+001	6.40E+001	6.35E+001	5.93E+001	4.75E+001	2.59E+001
	std	7.28E+000	4.88E+000	4.34E+000	2.95E+000	4.54E+000	3.26E+000
F10	mean	1.61E+000	6.32E–001	5.23E–001	1.72E+000	1.63E+000	2.89E–001

	std	1.00E–001	4.33E–001	4.20E–002	3.49E–001	2.69E–001	2.94E–001
F11	mean	4.46E+002	1.66E+002	2.68E+002	1.27E–013	4.70E+001	2.61E+002
	std	8.86E+001	3.12E+001	4.86E+001	2.45E–014	8.32E+000	9.85E+001
F12	mean	5.42E+002	2.97E+002	5.37E+002	8.46E+002	2.67E+002	2.46E+002
	std	1.25E+002	4.23E+001	1.06E+002	9.59E+001	5.81E+001	6.68E+000
F13	mean	6.35E+002	3.91E+002	5.59E+002	8.51E+002	4.46E+002	3.78E+002
	std	1.06E+002	4.82E+001	5.86E+001	7.03E+001	7.78E+001	9.18E+001
F14	mean	5.19E+003	7.22E+003	5.86E+003	1.95E+000	1.96E+003	3.99E+003
	std	8.45E+002	8.66E+002	1.01E+003	1.14E+000	3.56E+002	5.79E+002
F15	mean	7.81E+003	8.49E+003	8.32E+003	7.94E+003	7.76E+003	4.05E+003
	std	9.18E+002	1.16E+003	1.12E+003	6.22E+002	8.15E+002	8.59E+002
F16	mean	3.14E+000	2.66E+000	2.31E+000	2.60E+000	2.26E+000	2.03E+000
	std	5.48E–001	5.03E–001	6.10E–001	2.06E–001	2.91E–001	2.45E–001
F17	mean	6.35E+002	1.63E+002	4.04E+002	5.10E+001	1.42E+002	3.03E+002
	std	1.49E+002	2.81E+001	7.11E+001	5.25E–002	1.65E+001	3.55E+001
F18	mean	5.43E+002	1.61E+002	6.01E+002	7.84E+002	3.13E+002	3.99E+002
	std	1.27E+002	2.84E+001	1.35E+002	9.65E+001	6.45E+001	1.67E+002
F19	mean	3.93E+001	2.43E+001	3.78E+001	2.08E+001	1.78E+001	1.22E+001
	std	1.57E+001	6.29E+000	9.82E+000	1.63E–001	1.59E+000	1.47E+000
F20	mean	2.27E+001	2.09E+001	2.33E+001	2.45E+001	2.50E+001	1.50E+001
	std	1.13E+000	1.11E+000	9.70E–001	1.20E–001	4.64E–003	4.41E–011
F21	mean	9.30E+002	9.65E+002	7.83E+002	4.21E+002	9.27E+002	3.72E+002
	std	1.97E+002	2.48E+002	3.51E+002	1.19E+002	2.42E+002	8.29E+001
F22	mean	6.50E+003	9.49E+003	6.07E+003	3.20E+001	2.76E+003	4.46E+003
	std	1.20E+003	1.02E+003	1.23E+003	4.48E+000	6.05E+002	7.49E+002
F23	mean	9.72E+003	1.06E+004	1.03E+004	1.03E+004	8.53E+003	4.71E+003
	std	1.39E+003	1.08E+003	1.40E+003	7.63E+002	1.12E+003	7.30E+002
F24	mean	3.70E+002	3.20E+002	3.73E+002	3.77E+002	3.28E+002	2.88E+002
	std	1.73E+001	2.80E+001	1.28E+001	8.23E+000	1.44E+001	9.73E+000
F25	mean	4.18E+002	4.19E+002	3.94E+002	4.19E+002	3.53E+002	3.08E+002
	std	2.47E+001	2.22E+001	1.23E+001	8.21E+000	1.22E+001	8.32E+000
F26	mean	3.25E+002	3.14E+002	4.12E+002	2.62E+002	3.79E+002	2.15E+002
	std	1.27E+002	1.32E+002	1.07E+002	4.26E–001	8.17E+001	2.78E+000
F27	mean	1.87E+003	1.79E+003	2.00E+003	1.56E+003	1.52E+003	9.54E+002
	std	1.64E+002	2.81E+002	1.03E+002	7.11E+002	1.34E+002	6.69E+001
F28	mean	2.86E+003	6.31E+002	9.90E+002	4.00E+002	2.82E+003	3.24E+003
	std	2.37E+003	8.83E+002	1.54E+003	2.35E+001	1.48E+003	6.55E+002
F29	mean	4.00E+003	3.70E+003	3.50E+003	2.18E+003	1.33E+004	1.80E+003
	std	4.47E+003	1.76E+003	5.55E+003	2.67E+003	1.17E+004	1.52E+003
F31	mean	1.86E+004	5.07E+002	6.50E+002	2.84E+005	3.64E+002	3.13E+002
	std	5.67E+003	3.02E+002	2.06E+002	3.40E+004	1.01E+001	2.18E+000
F32	mean	6.92E+002	6.15E+002	6.73E+002	6.52E+002	6.47E+002	5.94E+002
	std	5.95E+001	4.85E+001	4.02E+001	2.60E+001	4.89E+001	3.38E+001
F33	mean	8.33E+002	7.02E+002	8.31E+002	7.14E+002	7.07E+002	8.43E+002

	std	4.45E+001	3.35E+001	7.63E+001	2.49E+001	4.22E+001	5.96E+001
F34	mean	6.45E+002	6.26E+002	6.50E+002	6.00E+002	6.07E+002	6.60E+002
	std	9.10E+000	4.79E+000	1.06E+001	8.44E+001	4.25E+000	1.81E+000
F35	mean	1.51E+003	8.67E+002	1.36E+003	9.29E+002	9.91E+002	7.46E+002
	std	1.74E+002	3.52E+001	1.17E+002	2.16E+001	4.40E+001	2.38E+000
F36	mean	1.14E+003	1.00E+003	1.14E+003	1.02E+003	9.97E+002	8.47E+002
	std	5.32E+001	3.74E+001	6.71E+001	2.57E+001	3.69E+001	1.64E+001
F37	mean	1.05E+004	3.18E+003	9.85E+003	6.65E+003	8.85E+003	9.00E+002
	std	2.33E+003	5.72E+002	1.85E+003	1.98E+003	4.15E+003	8.72E–001
F38	mean	7.40E+003	7.90E+003	8.20E+003	5.31E+003	7.17E+003	3.81E+003
	std	9.16E+002	7.80E+002	8.76E+002	4.06E+002	9.05E+002	2.84E+002
F39	mean	1.25E+003	1.27E+003	1.31E+003	2.38E+003	1.41E+003	1.00E+003
	std	3.28E+001	4.00E+001	6.32E+001	7.42E+002	7.36E+001	8.78E+000
F40	mean	1.39E+006	4.99E+005	3.32E+006	3.52E+006	6.85E+006	3.88E+005
	std	2.24E+005	2.63E+005	2.98E+005	1.53E+006	3.56E+006	1.79E+005
F41	mean	4.61E+003	4.03E+003	7.83E+003	4.40E+003	3.58E+004	2.52E+003
	std	3.66E+003	2.20E+003	7.61E+003	3.18E+003	1.07E+004	7.56E+002
F42	mean	2.60E+004	2.28E+004	3.40E+004	1.79E+006	1.20E+005	2.36E+004
	std	1.68E+004	8.65E+003	2.04E+003	1.37E+006	8.94E+004	2.16E+004
F43	mean	1.13E+004	4.56E+003	9.67E+003	1.15E+004	2.84E+004	2.32E+003
	std	6.33E+003	3.10E+003	6.73E+003	5.66E+003	8.58E+003	2.44E+002
F44	mean	3.37E+003	3.25E+003	3.63E+003	3.09E+003	3.14E+003	1.62E+003
	std	4.26E+002	3.34E+002	4.73E+002	2.41E+002	4.56E+002	2.68E+002
F45	mean	3.24E+003	2.97E+003	3.22E+003	2.73E+003	3.07E+003	3.01E+003
	std	3.69E+002	2.77E+002	3.94E+002	1.97E+002	4.04E+002	2.26E+002
F46	mean	1.41E+005	1.82E+005	9.65E+004	1.18E+006	9.11E+005	7.41E+004
	std	7.73E+004	2.39E+005	5.15E+004	6.42E+005	6.62E+005	4.26E+004
F47	mean	1.78E+004	1.99E+004	2.33E+004	2.97E+004	1.88E+004	1.66E+004
	std	9.89E+003	6.75E+003	8.74E+003	4.65E+003	1.74E+004	6.45E+003
F48	mean	3.22E+003	3.11E+003	3.38E+003	2.77E+003	3.00E+003	3.20E+003
	std	3.42E+002	2.88E+002	4.28E+002	1.56E+002	3.23E+002	1.59E+002
F49	mean	2.59E+003	2.49E+003	2.62E+003	2.54E+003	2.49E+003	2.75E+003
	std	4.90E+001	5.50E+001	6.46E+001	5.82E+001	4.03E+001	8.36E+001
F50	mean	9.20E+003	9.21E+003	9.90E+003	7.42E+003	8.52E+003	2.62E+003
	std	1.54E+003	2.06E+003	9.61E+002	4.50E+002	8.52E+002	8.62E+002
F51	mean	3.16E+003	2.99E+003	3.10E+003	2.98E+003	2.93E+003	3.86E+003
	std	1.20E+002	7.03E+001	9.85E+001	2.38E+001	4.41E+001	2.37E+002
F52	mean	3.35E+003	3.18E+003	3.29E+003	3.44E+003	3.11E+003	3.00E+003
	std	9.48E+001	7.04E+001	9.60E+001	1.70E+002	4.53E+001	2.93E+001
F53	mean	3.05E+003	3.08E+003	3.05E+003	3.06E+003	3.04E+003	3.01E+003
	std	4.02E+001	3.81E+001	3.84E+001	1.82E+001	3.42E+001	1.11E+001
F54	mean	8.24E+003	6.93E+003	8.73E+003	4.88E+003	5.60E+003	4.84E+003
	std	4.09E+003	6.35E+002	2.28E+003	1.69E+003	1.05E+003	3.36E+003
F55	mean	3.72E+003	3.65E+003	3.55E+003	3.37E+003	3.37E+003	4.83E+003

	std	1.44E+002	1.24E+002	1.25E+002	3.75E+001	6.83E+001	1.15E+003
F56	mean	3.29E+003	3.31E+003	3.30E+003	3.28E+003	3.30E+003	3.41E+003
	std	1.90E+001	1.99E+001	3.14E+001	1.45E+001	2.13E+001	2.43E+001
F57	mean	4.60E+003	4.51E+003	4.59E+003	4.38E+003	4.44E+003	4.22E+003
	std	4.33E+002	3.37E+002	4.37E+002	1.80E+002	3.40E+002	1.74E+002
F58	mean	1.96E+006	1.85E+006	1.92E+006	2.76E+006	1.81E+006	1.69E+006
	std	2.35E+005	1.04E+005	1.68E+005	7.07E+004	4.78E+005	4.91E+005

References

[1] M. R. Saad, M. M. Emam, M. E. Hosney, N. A. Samee, R. I. Alkanhel and E. H. Houssein. Fourier transform optimizer: A novel physics-inspired metaheuristic algorithm for optimization problems. *Knowledge-Based Systems.* 2026*,* 340, 115651.

[2] Deng, B. Baboon optimization algorithm: A novel nature-inspired metaheuristic algorithm for optimization problems. *Ain Shams Engineering Journal*. 2026, 6(17), 104178.

[3] E. Rashedi, H. Nezamabadi-Pour, S. Saryazdi, GSA: a gravity search algorithm. *Information Sciences*. 2009, 179 (13), 2232-2248.

[4] D. Chauhan and Shivani. Self-adaptive and locally-guided artificial electric field algorithm for global optimization with aggregative learning. *Knowledge-Based Systems.* 2025, 325, 113835.

[5] M. R. Narimani, A. A. Vahed, R. Azizipanah-Abarghooee and M. Javidsharifi. Enhanced gravity search algorithm for multi-objective distribution feeder reconfiguration considering reliability, loss and operational cost. *IET Generation, Transmission & Distribution.* 2014, 8(1),55-69.

[6] Lei, Z. Y., Gao, S. C., S. Gupta, Cheng, J. J. and Yang, G. An aggregative learning gravity search algorithm with self-adaptive gravity constants. *Expert Systems with Applications.* 2020, 152, 113396.

[7] H. Hendro, A. M. Shiddiqi and A. Saikhu. An enhanced gravity search algorithm for feature selection in telecom churn prediction. *Results in Engineering.* 2026, 30, 109989.

[8] N. Aditya and S. S. Mahapatra. An adaptive gravity search algorithm for optimizing mechanical engineering design and machining problem. *Engineering Applications of Artificial Intelligence.* 2024, 138, Part A, 109298.

[9] Qian, Z. Q., Xie, Y. F. and Xie, S. W. MAR-GSA: Mixed attraction and repulsion based gravity search algorithm. *Information Science*s. 2024, 662, 120250.

[10] Guo, A. J., Wang, Y. R., Guo, L. J., Zhang, R., Yu, Y. and Gao, S. C. An adaptive position-guided gravity search algorithm for function optimization and image threshold segmentation. *Engineering Applications of Artificial Intelligence.* 2023, 121, 106040.

[11] S. K. Joshi. Chaos embedded opposition based learning for gravity search algorithm. *Applied Intelligenc*e. 2023, 53, 5567-5586.

[12] C. Dikshit. Restart mechanism-based multilevel gravity search algorithm for global optimization and image segmentation. *Engineering Applications of Artificial Intelligence.* 2026, 163, Part 3,112904.

[13] Wang, Y. R., Yu, Y. and Gao, S. C. A hierarchical gravity search algorithm with an effective gravity constant. *Swarm and Evolutionary Computation.* 2017, 46, 118-139.

[14] Ji, J., Gao, S., Wang, S., Tang, Y. J. and Yu, H. Self-adaptive gravity Search Algorithm with A Modified Chaotic Local Search. *IEEE Access.* 2017, 6, 1-15.

[15] H. Mittal, M. Saraswat, R. Pal, A. K. Tripathi and A. C. Pandey. SGSA-C: a new spiky gravity search algorithm clustering method for segmentation. *International Journal of Machine Learning and Cybernetics.* 2025, 16, 8215-8235.

[16] S. Mirjalili and A. Lewis. Adaptive gbest-guided gravity search algorithm. *Neural Computing and Applications.* 2014, 25, 1569-1584.

[17] Vikas and D. R. Parhi. Chaos-based optimal path planning of humanoid robot using hybridized regression-gravity search algorithm in static and dynamic terrains. *Applied Soft Computing.* 2023, 140,110236.

[18] Chen, B. L., Wang, F. C. and Wang, H. C. Multi-strategy synergistically enhanced sand cat swarm optimization: Benchmark and engineering applications. *Advanced Engineering Informatics*. 2026, 71, 104255.

[19] Cheng M Y, Sholeh M N. Artificial satellite search: A new metaheuristic algorithm for optimizing truss structure design and project scheduling. Applied Mathematical Modelling, 2025, 143, 116008.

[20] Yang, K. W., Zhu, S. H. and Lu, S. F. Research on Three-Dimensional Path Planning of UAVs in Complex Terrain Based on Enhanced Grey Wolf Optimizer. *Procedia Computer Science*. 2026, 280, 110-117.

[21] R. R. Gurrala and S. K. Tallapally. A novel hybrid cheetah dung beetle optimization algorithm to solve cloud-fog scheduling problems. *Computers and Electrical Engineering.* 2026, 131, 110968.

[22] A. K. Mahto, M. A. Kalam and K. Paul. A novel hybrid Harris hawk optimization-sine cosine algorithm for the influence of electric vehicle and renewable energy sources in power system distribution network. *Franklin Open.* 2025, 13, 100401.

[23] Anita and A. Yadav. AEFA: Artificial electric field algorithm for global optimization. *Swarm and Evolutionary Computation.* 2019, 48, 93-108.

[24] M. Moslemzadeh, S. Farzin, and H. Karami. Introducing improved atom search optimization (IASO) algorithm: Application to optimal operation of multi-reservoir systems. *Physics and Chemistry of the Earth.* 2023, 131, 103415.

[25] Zhang, L. Adaptive diversity-driven multi-strategy particle swarm optimization for global optimization and feature selection. *Applied Soft Computing.* 2026, 201, Part A, 115525.

[26] Liu, J. S., Chen, Y. and Liu, X. Y. An efficient manta ray foraging optimization algorithm with individual information interaction and fractional derivative mutation for solving complex function extremum and engineering design problems. *Applied Soft Computing.* 2024, 150,111042.

[27] A. H. Gandomi. Interior search algorithm (ISA): a novel approach for global optimization. *ISA transactions.* 2014, 53(4), 1168-1183.

[28] Liu, J. S., Wu, H. and Li, Y. A multi-mechanism improved flow direction algorithm for solving wireless sensor networks coverage problem in complex scenarios. *Expert Systems with Applications.* 2026, 301, 130483.

[29] Zhang, Z. L., Zhou, X. Y.and Song, J. Y. Adaptive exploration-exploitation switching artificial bee colony algorithm based on problem features. *Expert Systems with Applications.* 2026, 318, 131979.

[30] Tian, L. J., Niu, C. and Wang, X. An improved slime mould algorithm applied to hyperspectral feature selection in soil fertility indicators. *International Journal of Applied Earth Observation and Geoinformatio*n. 2026, 152, 105395.

[31] Gu, T. H., Li, Y. L. and Wang, C. X. Urban multi-task path planning for UAV swarms based on the multi-strategy enhanced black-winged kite algorithm. *Expert Systems with Applications.* 2026, 331, 133269.

[32] Zhang, W. and Mo, Y. B. Multi-strategy improved partial reinforcement optimization algorithm for UAV path planning. *Applied Soft Computing.* 2026, 201, 115577.

[33] Wang, M. B., Chen, C. C. and Liu, J. T. ADSESC: An enhanced escape algorithm based on adaptive decentralized search strategy for low-altitude UAV path planning in complex environments. *Applied Soft Computing.* 2026, 200, 115390.